CRANFIELD UNIVERSITY

Yuqing Qiao

Effect of Wing Flexibility on Aircraft Flight Dynamics

School of Engineering
MSc by Research

MSc Thesis
Academic Year: 2011 - 2012

Supervisor: Dr Alastair Cooke
Feb. 2012

CRANFIELD UNIVERSITY

School of Engineering
MSc by Research

Full Time MSc

Academic Year 2011 - 2012

Yuqing Qiao

Effect of Wing Flexibility on Aircraft Flight Dynamics

Supervisor: Dr Alastair Cooke
Feb. 2012

This thesis is submitted in partial fulfilment of the requirements for the degree of Master of Science

ABSTRACT

The purpose of this thesis is to give a preliminary investigation into the effect of wing deformation on flight dynamics. The candidate vehicle is FW-11 which is a flying wing configuration aircraft with high altitude and long endurance characteristics. The aeroelastic effect may be significant for this type of configuration. Two cases, the effect of flexible wing on lift distribution and on roll effectiveness during the cruise condition with different inertial parameters are investigated.

For the first case, as the wing bending and twisting depend on the interaction between the wing structural deflections and the aerodynamic loads, the equilibrium condition should be calculated. In order to get that condition, mass, structure characteristics and aerodynamic characteristics are estimated first. Then load model and aerodynamic model are built. Next the interaction calculation program is applied and the equilibrium condition of the aircraft is calculated. After that, effect of wing flexibility on lift parameters is investigated. The influence of CG, location of lift and location of flexural axis are investigated.

The other case is to calculate the transient roll rate response and estimate the rolling effectiveness of flexible aircraft, and compared with the rigid aircraft's. A pure roll model is built and derivatives both for the rigid wing and the flexible wing are estimated. It has been found that flexible wing leads to the loss of control effectiveness, even cause reversal when reduces the structure natural frequency. The influence of inertia data for flexible roll is also investigated.

Keywords:

Static aeroelasticity, wing deformation, lift distribution, roll effectiveness

ACKNOWLEDGEMENTS

I would like to express my great appreciation to my supervisor, Dr Alastair. Cooke, for his great support throughout this project. I also thank Dr S. Guo and his student Daqing. Yang and Laibin. Xu, for their help along this project.

Also, I give my gratitude to CAIGA , AVIC and CSC who have provided me with the opportunity to study in Cranfield University.

Moreover, I would like to express my great appreciation to my family and friends. Thanks for their unending support.

TABLE OF CONTENTS

LIST OF FIGURES

LIST OF TABLES

LIST OF ABBREVIATIONS

AC	Aerodynamic Centre
AoA	Angle of attack
AR	Aspect ratio
BWB	Blended Wing Body
CG	Centre of Gravity
CP	Centre of Pressure
CFD	Computational Fluid Dynamics
DoF	Degree of freedom
EI	Bending stiffness
ESDU	Engineering Science Data Unit
FW	Flying Wing
GJ	Torsional stiffness
GDP	Group Design Project
MTOW	Maximum Takeoff Weight
Ma	Mach number
TE	Trailing Edge

LIST OF NOTATION

ξ	Aileron angle perturbation
C_D	Drag coefficient
c_e	Damping ratio of the flexible torsion mode
Q_p	Flexible mode generalized force due to the roll rate
Q_ξ	Flexible mode generalized force due to the deflection of the aileron
Q_e	Flexible mode generalized force due to flexible mode deformation
a_w	Lift curve slope with modified strip method
$\alpha_{(y)}$	Local angle of attack along the spanwise direction
C_L	Lift coefficient
c	Length of the mean chord
I_x	Moment of inertia roll
m_e	Model mass of the flexible torsion mode
C_M	Pitching moment coefficient
k_e	Stiffness of the flexible torsion mode
L_p	Rolling moment derivative due to the roll rate
L_ξ	Rolling moment derivative due to aileron
L_e	Rolling moment due to flexible mode deformation
Re	Reynolds number
α_e	Trimmed angle of attack

1 Introduction

1.1 Aim and Objectives

The aim of this thesis is to give a preliminary investigation into the effect of wing deformation on flight dynamics. The candidate vehicle is FW-11 which is a flying wing configuration aircraft with high altitude and long endurance characteristics. The aeroelastic effect may be significant for this type of configuration. The effect of flexible wing on lift distribution and on roll effectiveness is investigated. The results of this method can be used as reference data to optimize the structure and control system when FW-11 comes to the preliminary design stage.

This thesis presents a preliminary method to calculate the static aeroelasticity deformation and the rolling effectiveness of flexible aircraft, which includes the structure part, aerodynamic part and flight dynamic part.

To achieve the aim of the project, these objectives below should be implemented.

1. Development of loads model:
   Calculate mass distribution first. Then estimate the structure characteristics like the stiffness of the wing.
2. Development of aerodynamic model
   Estimate the aerodynamic characteristics and use the modified strip method to calculate the aerodynamic forces and moments.
3. Development of deformation model:
   Do the interaction calculation between the load model and the aerodynamic model. It is the interaction between the wing structural deflections and the aerodynamic loads in more specific terms and the equilibrium condition of the aircraft is achieved. Then estimate the effect of wing flexibility on lift distribution.
4. Evaluation of flight dynamic characteristics:
   Build the roll model of the aircraft, calculate the transient response and estimate the rolling effectiveness of flexible aircraft, and compare with the rigid aircraft's.

1.2 Background

FW-11 is a group design project between Cranfield University and AVIC (Aviation Industry Corporation of China). It is a conceptual design of flying wing commercial aircraft with 250 seats and 7500 nautical miles range. Figure 1-1 shows the general appearance of FW-11.

Figure 1-1 FW-11 [1]

The flying wing configuration is one of the next generations of high altitude, long endurance vehicles. Now, the conception becomes more and more popular due to its high aerodynamic efficiency. It consumes less fuel, which means lower cost for people to travel and more environment friendly.

As FW-11 is a high altitude and long range aircraft, the wing probably has quite different deformation shape than the undeformed shape. The wing bending and twisting depend on the interaction between the wing structural deflections and the aerodynamic loads. The deformation is calculated first. After that the spanwise lift distribution is estimated. Then the transient response of a pure roll case and the rolling effectiveness of flexible aircraft are calculated and the results are compared with the rigid aircraft's.

1.3 Report Overview

In chapter 2, a literature review is provided about the related topics as the flying wing, aeroelasticity and previous related researches. In chapter 3, the related governing equations of the structure, aerodynamics and flight dynamics are

given. In chapter 4 and chapter 5, the loads model and the aerodynamic model are developed. In chapter 6, the deformation model is built and the effect of wing flexibility on lift distribution is investigated. In chapter 7, some effects of aeroelasticity on the rolling effectiveness are estimated. Followed that, conclusions and future work are given in chapter 8 and chapter 9. Last are the references and appendices.

2 Literature review

2.1 Flying wing configuration

Flying wing, as a new idea to improve the efficiency of aviation technology, is one of the most interesting topics and has drawn much attention during the past 20 years [2].

Flying wing is an unconventional configuration and is defined as a tailless aircraft which can accommodate all the parts within the outline of a single airfoil [3]. Each section across the spanwise direction of the wing is designed airfoil and can generate lift. The cabin and the cargo are also located in the wing area. Flying wing has the significant benefits on higher lift drag ratio, lower weight and lower fuel consumption.

Blended wing body (BWB) configuration is unavoidable when considering the flying wing because the inherent relation between the two concepts. BWB has the definition of a concept where fuselage is merged with wing and tail to become a single entity. To some extent, BWB can be considered as an evolution concept or a special branch of flying wing. Some researchers advocate the idea of hybrid flying wing to distinguish the two configurations. They suggest three types of configurations: pure flying wing, hybrid flying wing and blended-wing-body configurations.

Three flying wing aircrafts are introduced here, XB-35 (Figure 2-1), YB-49 (Figure 2-2) and B-2 (Figure 2-3).

The XB-35 (Figure 2-1) was designed by the Northrop Corporation for the USA Army Air Forces as a heavy bomber, shortly after the Second World War. It was designed to be a potentially efficient flying wing configuration, using piston engine. It has a wing span of 52.2m, total length 16.2m, wing area 370m^2, and maximum takeoff weight 95,000Kg. The XB-35 uses elevon to replace the elevator and aileron on conventional aircraft, and other multifunctional control surfaces. In June 1946, the XB-35 made her first flight for 45 minutes with no problems, but only prototype and pre-production aircraft were built [4].

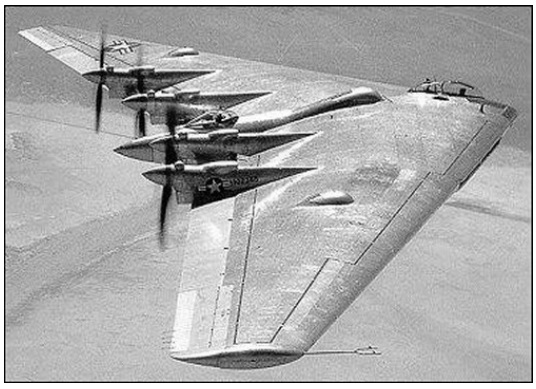

Figure 2-1 XB-35 bomber [4]

The YB-49 (Figure 2-2) was a prototype jet-powered heavy bomber, converted from the YB-35 test aircraft. The most distinct difference was the powerplant system, and four small vertical fins were added on YB-49 to augment weathercock stability lost with the removal of the propeller shaft housing. YB-49 performed its first flight on 4 February 1949 for 4 hours 25 minutes. The project was ended in 1950 and it never entered production [4].

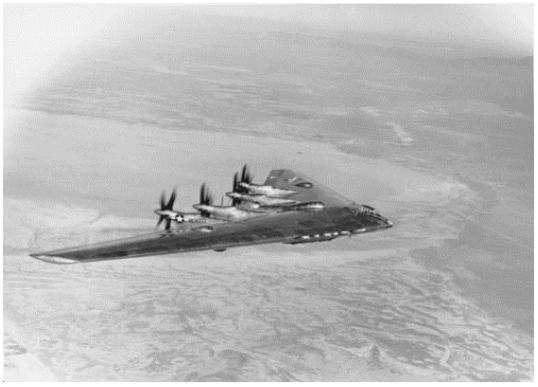

Figure 2-2 YB-49 bomber

Although both XB-35 and YB-49 were not successful, however, the design work by Northrop in the development process was proved to be useful for the following design of the B-2 Spirit strategic bomber. The B-2 was designed to penetrate dense anti-aircraft defenses, using low observable stealth technology which combine the reduced acoustic, infrared, visual and radar signatures. It was clear that the flying wing configuration contributes significantly to its stealth characteristics, with composite materials, special coatings, etc. The flying wing design also provided the B-2 with one remarkable advantage over previous

bombers: Its range was reported as 6,000 nautical miles with cruise speed at M 0.85 [5].

Figure 2-3 B-2 bomber [5]

2.2 Aeroelasticity

Aeroelasticity describes the interaction between aerodynamic forces, inertia forces and elastic forces for a flexible aircraft structure and the phenomena that can result [6].

2.2.1 Static aeroelasticity

Static aeroelasticity is the study of the deflection of flexible aircraft structure under aerodynamic loads, where the forces and motions are considered to be independent of time [7].

The assumption that aerodynamic lift and moment only depend on the angle of attack of each strip is made. These loads and inertia loads cause the bending and twisting of the wing. These deformations also change the angle of attack and consequently change the aerodynamic flow. There is an interaction between the forces and the deflections until an equilibrium condition is reached.

The interaction between the wing structural deflections and the aerodynamic loads determines the wing bending and twisting at each flight condition, and must be considered in order to model the static aeroelastic behaviour. The static aeroelastic deformations are important as they govern the loads in the steady flight condition, the lift distribution, the drag forces, the effectiveness of

the control surfaces, the aircraft trim behaviour and also the static stability and control characteristics.

There are two critical static aeroelastic phenomena that can be encountered, namely divergence and control reversal.

2.2.1.1 Divergence

Divergence is the name given to the phenomenon that occurs when the moments due to aerodynamic forces overcome the restoring moments due to structural stiffness, so resulting in structural failure. The most common type is that of wing torsional divergence. On a historical note, it is thought that Langley's attempt to fly some months before the Wright Brothers' successful flights in 1903 failed due to the onset of divergence [8]. When the Langley aircraft was rebuilt some years later by Curtis with a much stiffer wing structure, the aircraft flew successfully. In general, for aeroelastic considerations the stiffness is of much greater importance than the strength. In modern aircraft, the flutter speed (the air speed at which flutter, a dynamic aeroelastic instability) is usually reached before the divergence speed (the air speed at which divergence occurs), so divergence is not normally a problem [9].

2.2.1.2 Control reversal

The effect that aeroelastic deflections of the flexible wing have influence on effectiveness of control surfaces in comparison to the rigid wing is considered. It is shown that as the speed increases the effectiveness reduces until at some critical speed which is called the reversal speed [8] (There is no response to application of the control surface). At speeds greater than the reversal speed, the action of the controls reverses, a phenomenon known as control reversal. Although not necessarily disastrous, it is unacceptable that at speeds near to the reversal speed, the aircraft responds either very slowly or not at all to application of the controls, and that the opposite response to that demanded occurs beyond the reversal speed

2.2.2 Dynamic Manoeuvres

Aircraft are controlled by the pilot using the control surfaces (namely aileron/spoiler for roll, rudder for yaw and elevator for pitch) singly or in combination for a range of different manoeuvres. The structure must be designed to withstand these manoeuvres and these load calculations are a critical stage in the aircraft clearance, often involving many thousands of cases. A useful background to meet most of the loads requirements in the certification specifications (CS-25 and FAR-25) is given in reference [10]. In this thesis, the process of calculating the transient response and estimating the rolling effectiveness in a pure roll manoeuvre is considered, using a progression of fairly basic mathematical models for both rigid and simple flexible aircraft. The flexible aircraft needs to be considered since flexibility can affect the loads distribution; CS-25 states: 'If deflections under load would significantly change the distribution of internal or external loads, this redistribution must be taken into account'. In effect, this is a statement that aeroelastic effects must be accounted for in loads calculations. The ability to correct the rigid aircraft derivatives for flexible effects are also be considered. Note that the axes system used in this thesis are inertial, i.e. earth fixed, and the unknowns are displacements and angles.

2.3 ESDU VGK method

VGK is a CFD (computational fluid dynamics) method coded for estimating the aerodynamic characteristics of an airfoil [11]. It is coded in FORTRAN and suitable for subsonic aircraft (In this method, the range of Mach number from 0.05 to 0.95). The effects of viscosity (boundary layers and wake) and compressibility are considered. VGK uses an iterative approach to solve coupled finite-difference equations for the inviscid flow region and the viscous flow region (represented by integral equations).

VGK is a computational method for determining two-dimensional transonic attached flow past a lifting aerofoil immersed in a subsonic free stream, with allowance for viscous effects. The method couples finite-difference solutions of inviscid flow about the aerofoil with solutions for the displacement effects of the boundary-layer and wake. The boundary conditions for the inviscid flow element employ a non-zero normal velocity at the aerofoil surface to allow for the growth of the boundary-layer displacement surface, and a jump in velocity across the dividing streamline to allow for wake thickness and curvature effects. The viscous flow element consists of integral methods for the laminar and turbulent boundary-layer components, and the displacement and momentum thickness distributions are calculated allowing for the effects of the pressures obtained from the inviscid flow element. The method of coupling the viscous and inviscid flow elements in VGK permits converged solutions to be obtained by iterative procedures for flows with attached boundary layers.

2.4 Previous related researches

There are some experiments researches that deal with the effects of aeroelasticity on the control surfaces. For example, the Langley Pilotless Aircraft Research Division made an investigation to determine some effects of aeroelasticity on the rolling [12] effectiveness of a 1/11-scale of the Bell X-5 aircraft wing at zero angle of attack. Rolling effectiveness was obtained over a range of Mach number from 0.6 to 1.5.The results indicated that severe rolling

effectiveness losses because of the wing flexibility even caused control reversal at subsonic speed.

There are also some computer-aid simulation researches that deal with flexible wings. Bonnet ([13]) did the research on aeroelastic deflection; he concentrated on the trailing edge deflection and tried to find a reasonable set of loads to get an ideal deflected shape for drag reduction and pitching moment effectiveness. His research is also included a structure and an aerodynamic part. Yan ([14]) used one CFD/CSD coupled method to calculate the static aeroelastic deformation of the wing and estimated the effect of flexible wing on longitudinal static margin.

3 Equations

3.1 Elastic bending and twisting

In this subsection, basic formulas of beam bending and twisting are introduced, based on reference [15], and prepared to use in the interaction with aerodynamic forces.

3.1.1 Elastic bending

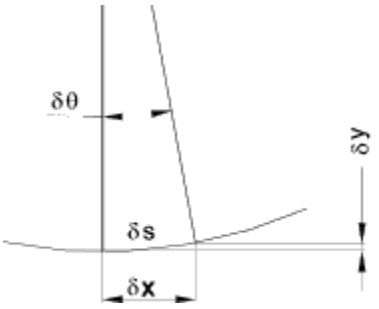

Figure 3-1 Elastic bending

Base on the small bending angle, as in Figure 3-1, beam is bending in x axis.

Bending curvature $\frac{1}{R}=\frac{d\theta}{ds}=\frac{d\theta}{dx}=\frac{d}{dx}(\frac{dy}{dx})=\frac{d^2y}{dx^2}$ (3-1)

where R is the curvature of a beam, θ is the slope of bending deflection, x is the bending deflection, y is the neutral axis of the beam.

Bending slope $\theta=\frac{dy}{dx}=\int(\frac{d^2y}{dx^2})dx=\int\frac{M}{EI}dx$ (3-2)

where M is the bending moment, EI is the bending stiffness

Bending deflection $x=\int\theta dx=\iint\frac{M}{EI}dx$ (3-3)

3.1.2 Elastic twisting

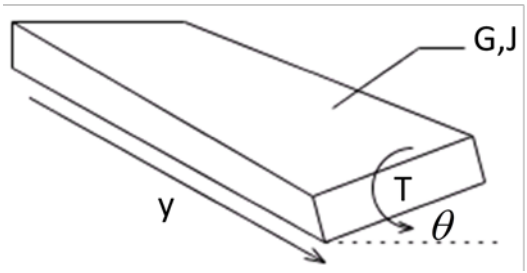

Figure 3-2 Elastic twisting

In Figure 3-2, twisting angle $\theta = \int \frac{T}{JG} dy$ (3-4)

where θ is the torsion angle, T is the torsion moment, GJ is the torsion stiffness.

3.2 Forces on an airfoil

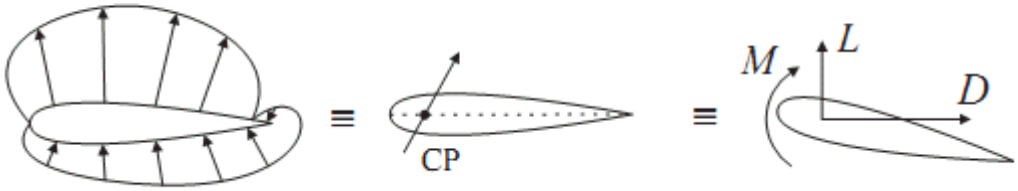

Figure 3-3 Resultant aerodynamic force acts at the centre of pressure

When an aerofoil moving at velocity V in a fluid, the pressure distribution acting over the surface of the aerofoil gives rise to a total force. The position on the chord at which the resultant force acts is called the centre of pressure, as shown in Figure 3-3. If the angle of attack α (angle between the mean airflow and the chord line of the aerofoil) changes, then the pressure distribution over the aerofoil changes, which leads to a repositioning of the centre of pressure. The changing centre of pressure position with respect to different angles of incidence leads to difficulties in any simple aeroelastic analysis, since the forces and moments need to be recalculated continually. For convenience, the net force is usually replaced by two resultant orthogonal forces, acting at a chosen reference point on the aerofoil, and a moment as seen in Figure 3-3.

The lift (L) is the force normal to the relative velocity of the aerofoil and fluid, the drag (D) is the force in the direction of relative velocity of the aerofoil and fluid, and the pitching moment (M) is the moment due to offset between the centre of pressure and the reference point (as shown in Figure 3-3). It is usual to use coefficients which relate the above quantities to the dynamic pressure and chord for a unit span of aerofoil (since it is two-dimensional), so that the lift, drag and moment coefficients are defined respectively as [9]

$$C_L = \frac{L}{\frac{1}{2}\rho V^2 c} \quad \textbf{(3-5)}$$

$$C_D = \frac{D}{\frac{1}{2}\rho V^2 c} \quad \textbf{(3-6)}$$

$$C_M = \frac{M}{\frac{1}{2}\rho V^2 c^2} \quad \textbf{(3-7)}$$

where c is the aerodynamic aerofoil chord and lift, and drag and pitching moment are defined per unit span of the aerofoil.

3.3 Strip theory

In the strip theory, the wing is considered to be composed of a number of elemental chordwise ‘strips’ and it is assumed that the lift coefficient on each chordwise strip of the wing is proportional to the local angle of attack $\alpha_{(y)}$ and that the lift on one strip has no influence upon another. Consider the kth ‘strip’ (or section) located at a distance of y_k from the root and chord c as shown in Figure 3-4.

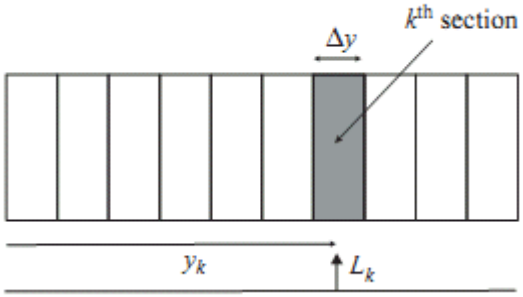

Figure 3-4 Strip theory

The lift force acting upon the kth strip is [16]

$$\mathrm{L_k} = \frac{1}{2}\rho V^2 c \,\Delta\, y a_1 \alpha_{(y)} \tag{3-8}$$

3.4 Modified method for lift distribution

There are a number of simple adjustments that can be made to the value of the lift curve slope for a two-dimensional aerofoil in order to account approximately for finite span wings and also the effects of compressibility. For three-dimensional finite span wings, the value of the lift curve slope is given the symbol α_w. The strip theory may be modified to account for the reduction towards the tip. The lift curve may be varied along the spanwise direction, with lift falling off to zero at the wing tips. Then the effective wing lift curve slope can be shown to take the form Yates [17].

$$a_{\mathrm{w}}(\mathrm{y}) = a_1 \cos\left(\frac{\pi \mathrm{y}}{2\mathrm{s}}\right) \tag{3-9}$$

The local chord could have been used for a tapered wing and the lift curve slope a_1 is corrected in the equation above. Thus the total lift on the single wing would be given by equation 3-10.

$$\mathrm{L_{total}} = \sum \frac{1}{2}\rho V^2 c_{(y)} \,\Delta\, y a_1 \alpha_{(y)} \tag{3-10}$$

3.5 Rigid aircraft in roll

The torsion mode for the simplified pure roll case is considered. For a rigid aircraft it is one DoF model. Wright and Cooper [9] and Lomax [10] make a

similar assumption for neglecting cross-coupling effects, for consideration of dynamic rolling manoeuvres. Although this approach is somewhat crude, it may be still essentially rational for preliminary investigation into the effect of wing deformation on flight dynamics.

Before apply the ailerons, the aircraft is assumed to be in straight and level trimmed flight. After applying the ailerons, the aircraft is assumed to roll with an angular velocity p (positive starboard wing down), angular acceleration $\dot{p}$ and transient roll angle ϕ. There are no yaw or sideslip motions for this pure roll case.

The linear flight mechanics equations of motion for the lateral case of symmetric aircraft, for small rates of rotation, from Cook [18], to be

$$m(\dot{v} - W_e p + U_e r) = Y \quad \textbf{(3-11)}$$

$$I_x \dot{p} - I_{xz} \dot{r} = L \quad \textbf{(3-12)}$$

$$I_z \dot{r} - I_{xz} \dot{p} = N \quad \textbf{(3-13)}$$

Wing axes is chosen and it is assumed that the product moment of inertia I_{xz} may be set to zero to avoid inertia coupling. Thus the equations of the motion may be rewritten as

$$m(\dot{v} + U_e r) = Y \quad \textbf{(3-14)}$$

$$I_x \dot{p} = L \quad \textbf{(3-15)}$$

$$I_z \dot{r} = N \quad \textbf{(3-16)}$$

Clearly the yawing moment N and side force Y must both be zero so as to avoid yaw and sideslip responses and therefore any aerodynamic couplings to roll motion must also be ignored. Thus the equation governing the simplified aircraft motion is simply the roll equation

$$I_x \dot{p} = L \quad \textbf{(3-17)}$$

The rolling moment L may be expressed in terms of aerodynamic stability derivatives [18], namely

$$L = L_p p + L_\xi \xi \tag{3-18}$$

where L_p and L_ξ are rolling moments due to roll rate p and aileron angle ξ respectively, defined here in wind axes, which is estimated in section 7, and other terms involving the null yaw and sideslip motions are omitted. Then the equation of motion is

$$I_x \dot{p} - L_p p = L_\xi \xi \tag{3-19}$$

and this equation may be used to determine the response to any aileron input.

3.6 Flexible aircraft in roll

The investigation into the pure roll behaviour of the flexible antisymmetric wing torsion mode is applied. This method considered that the wing is flexible in twist but rigid in bending. The motion of the flexible rolling aircraft may then be represented using a combination of rigid body roll motion and a flexible antisymmetric mode with a twist variation along the wing (defined nose up on the starboard wing is positive direction).It is considered that the deflection of the airfoil is linear along the spanwise, and a variable $\gamma_e(y)$ is introduced ($\gamma_e(y)$ =y/s). The wing twist due to the flexible deformation at position y is $\gamma_e(y)q_e$.

Two assumptions are made in deriving the mean axes approximations and eliminate inertia coupling terms between the rigid and flexible equations. One is assumed the centre mass remains in the same location, relative to the body axes at all time. The other is assumed that the relative angular momentum is zero. The advantage of the mean axes is that any inertia coupling terms between rigid and flexible equations are zero or may be neglected; thus the kinetic energy expression is considerably simplified, having separate rigid and flexible terms. Thus the flight dynamic equations of motion for the flexible aircraft in roll are [9]

$$I_x\dot{p} = L \tag{3-20}$$

$$m_e\ddot{q}_e + c_e\dot{q}_e + k_e q_e = Q_{ext} \tag{3-21}$$

where m_e, c_e, k_e, Q_{ext} are the modal mass, damping, stiffness and external force respectively for the antisymmetric torsion mode.

Because of limited time, the torsion mode shape is assumed to be linear. According to the simple estimation from Wright and Cooper [9],

$$T = \frac{1}{2}m_e\dot{q}_e^2 = 2 * \frac{1}{2}\int_0^s \chi_w\,[\gamma_e(y)\dot{q}_e]^2 dy \tag{3-22}$$

where χ_w is the wing torsional moment of inertia in pitch per unit span about the wing mass axis.

The modal mass may be expressed as

$$m_e = 2 * \int_0^s \chi_w\,[\gamma_e(y)]^2 dy = \frac{I_w}{3} \tag{3-23}$$

The rolling moment and generalized force may be written in derivative form as [9]

$$L = L_p p + L_\xi \xi + L_e q_e \tag{3-24}$$

$$Q_{ext} = Q_p p + Q_\xi \xi + Q_e q_e \tag{3-25}$$

where L_p and L_ξ are the same as for the rigid aircraft. The other derivatives are associated with the flexible deformation of the aircraft. For example, L_e is the rolling moment due to flexible mode deformation and Q_p is the flexible mode generalized force due to the roll rate. The derivatives are calculated in chapter 7.

4 Development of loads model

4.1 Introduction

At first, the assumption that the inner wing is rigid and has no flexibility is made. Compared with the outer wing, the deformation of the inner wing is very small and can be ignored. Also, it makes the process of building the load and deformation model much simpler.

Secondly, the cruise flight at 30,000 feet at Mach number 0.8 is chosen as the flight condition, as the aircraft has most of the time at this condition.

After that, build the outer wing as a beam model. It is quite common to use beam model in the static aeroelastic analyse. The wing is symmetric, so in this thesis, the starboard wing is chosen to build the entire load and deformation model.

4.2 Elementary geometry data

In order to use the strip method to calculate the aerodynamic forces, the first step is to divide the outer wing into several elementary sections, from tip to root. Based on the dimensions of the model [19] (the wingspan is 16 m), the summary of the strip areas is below (y is the distance to the root of the outer wing, S is the area of each section):

Table 4-1 Geometry data of each strips

Section	y(m)	S(m^2)
1	0-2	11.5
2	2-4	10.5
3	4-6	9.5
4	6-8	8.5
5	8-10	7.5
6	10-12	6.5
7	12-14	5.5
8	14-16	4.5

4.3 Mass distribution

FW-11 is an aircraft of flying wing configuration, so the method to predict the mass especially the mass of airframe is quite different from the conventional aircraft. The author uses the “F” method from Howe, D [20] to predict the airframe mass. Applying this method to FW-11, the aircraft is divided into two parts, the inner wing and the outer wing. The inner wing carrying the payload as passengers and cargos has both wing function and fuselage function, and the outer wing carrying outboard fuel tank has only wing function. The method also considered penalties for the secondary structure. Based on the estimation of structure mass and combined the mass prediction method from Cranfield teaching notes [21], the maximum take-off weight and its breakdown items can be estimated. The moment of inertia in roll is calculated in preparation for use in chapter 7.

In the outer wing, three parts of mass are included: the structure mass, the systems mass and the fuel mass. According to the mass data from GDP [22], let the structure mass and systems mass evenly arrange to the area of each section. Two cases of mass distribution are considered. One is outer wing with full fuel, for which CG of the outer wing is 35% at MAC of the outer wing. The other is outer wing without fuel, for which CG is 32% at MAC. Table 4-2 and 4-3 show the mass distribution of the outer wing for the two different CG situations which are the situations at the beginning and the end of the cruise flight.

Table 4-2 Mass distribution CG=35% MAC

	mass	unit
m1	1071	kg
m2	795	kg
m3	673	kg
m4	561	kg
m5	460	kg
m6	368	kg
m7	70	kg
m8	14	kg

Table 4-3 Mass distribution CG=32% MAC

	mass	unit
m1	749	kg
m2	557	kg
m3	471	kg
m4	392	kg
m5	322	kg
m6	257	kg
m7	70	kg
m8	14	kg

4.4 Stiffness calculation

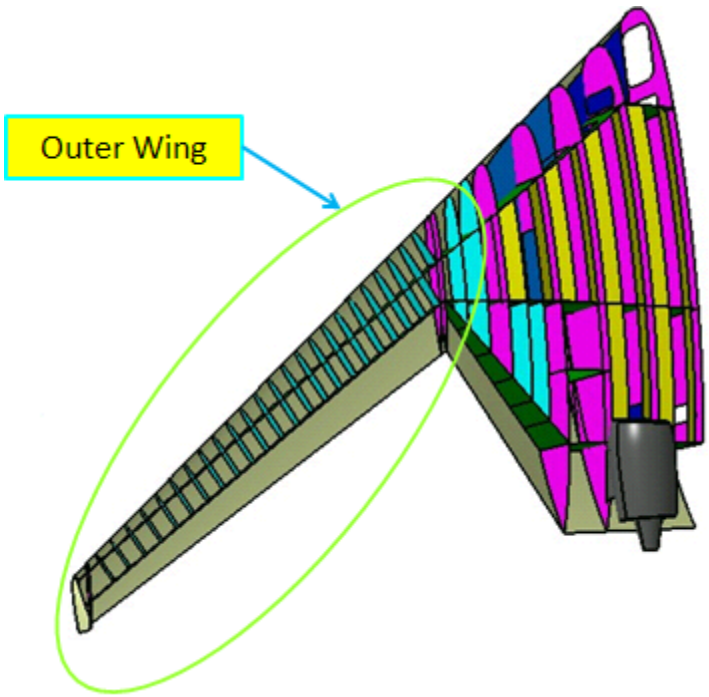

Figure 4-1 Structure layout of the outer wing of FW-11

- The layout of spar

As illustrated in Figure 4-1, the front spar is at 14% chord and rear spar is at 65%.

- Build the beam model

Use the geometry data of outer wing from CATIA model [19]. As the root of the outer wing is fixed, it is a cantilever beam model. For the beam structure, only

consider the beam box, which is the main part to carry forces and moments. The beam is divided into 8 sections with equal distance in the spanwise direction, the same as the elementary geometry data.

- Calculate the length of the chord as below

$$c(y) = \frac{c0 - c8}{L} \quad \textbf{(4-1)}$$

where c0 is the length of the root chord, c8 is the length of the tip chord, L is the length of the starboard wing, and consider it is linear in the spanwise direction.

- Choice of materials

As FW-11 is in a conceptual stage, many details of the structure are not completed. The author chooses AS4/3501-6 (Carbon-Epoxy prepreg) as the material for the beam model. It is one of the common materials for large commercial aircraft. The material property is shown below.

Table 4-4 Material property of AS4/3501-6

Density(kg/m^3)	1600
Longitudinal Modulus,E1 (GPa)	142
Transverse Modulus,E1 (GPa)	10.3
In-plane Shear Modulus,G12(GPa)	7.2
Poisson ratio	0.27

- Estimate stiffness matrix

Calculate the stiffness matrix with the cranfield in house programme BOXMXESC [23], which is a Programme to produce composite [ABD] matrix and the bending and torsional stiffness parameters of a composite-box beam.

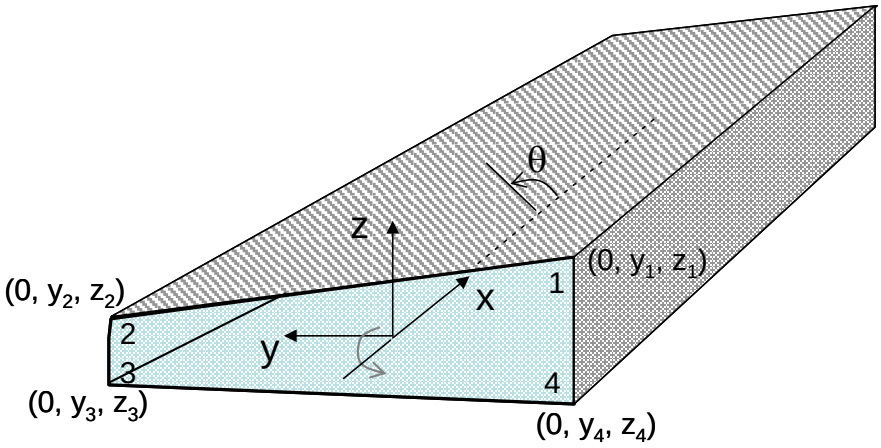

Figure 4-2 Coordinate of the beam

The coordinate of the beam model is illustrated in the Figure 4-2. Here y-axis is different from other places in this thesis which y-axis is the spanwise direction, as it is the requirement of the program. The input data is shown in the Table 4-5.

Table 4-5 Input data of one section

Number of parts divided for loop integral	4
unit system	SI unit
Number of Layers	8
Fiber direction	0,90,0,45,-45,0,90,0
Thickness	0.25E-3 0.25E-3 0.25E-3 0.25E-3 0.25E-3 0.25E-3 0.25E-3 0.25E-3
The x,y,z coordinates of the nodes	(0,-1.8,0.3) (0,1.8,0.3) (0,1.8,-0.3) (0,-1.8,-0.3)

Table 4-6 shows the stiffness of some sections.

Table 4-6 Stiffness of the beam

	EI	GJ
Section 1	0.40310E+09	0.50920E+09
Section 4	0.19010E+08	0.31388E+08
Section 8	0.42284E+07	0.61165E+07

Consider it is linear in the spanwise direction.

5 Development of aerodynamic model

5.1 Introduction

The purpose is to determine aerodynamic parameters for the airfoil in the steady flight condition, which is at Mach number 0.8 at 30000 feet altitude. Several programs can be used for this estimation, like AVL [24], xfoil [25] and ESDU VGK method [26]. The author run one simple example in xfoil and found xfoil can not consider the compressibility at such speed. As the outer wing has been divided into several sections, the aerodynamic character of airfoil is concerned. AVL can not estimate the parameter of the airfoil. The ESDU method is used to calculate the aerodynamic parameters.

Outer wing airfoil is NACA Langley RC-SC2, which is supercritical airfoil with high speed performance [27]. Figure5-1 below illustrates the geometry of the airfoil.

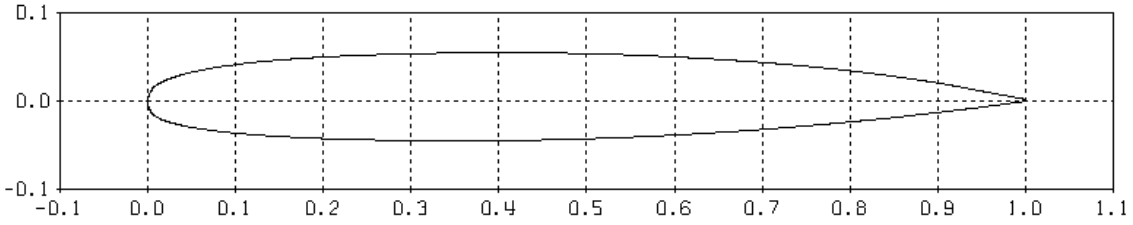

Figure 5-1 Airfoil RC-SC2

5.2 Basic parameters

- Velocity for cruise condition

  The cruise altitude is 10,000m. According to an atmospheric model [28], basic aerodynamic parameters at this altitude are shown below

Table 5-1 Basic aerodynamic parameters

T	223.15 K
P	26436.26 Pa
ρ	0.38 Kg/m^3
a	299.46 m/s

where T is temperature, P is pressure, ρ is density and a is speed of sound

The cruise Mach number is 0.8, according to the aerodynamic data from GDP.

$$V = Mach \times a \tag{5-1}$$

The velocity value in the steady flight condition V equals 240 m/s.

- Reynolds number with a velocity of 240 m/s, Re=5e8

$$Re = \frac{\rho V c}{\nu} \tag{5-2}$$

5.3 Procedure

A. Aerodynamic characteristics for a static aeroelasticity analyse

Use ESDU-w0315 (VGK method for windows) [29] to calculate the aerodynamic characteristics of a two-dimensional single-element aerofoil in a subsonic free stream. Table 5-2 and 5-3 are one example of the input parameters and initial settings for the program.

Table 5-2 Input parameters of VGK

Analysis type	viscous
Freestream mach number	0.8
Required starting incidence	0 deg
Reynolds number	5e8
Upper surface transition location	0.05
Lower surface transition location	0.05

Table 5-3 Initial settings of VGK

Number of radial mesh grid lines in the fine grid	160
Number of coarse mesh iterations for the inviscid flow	100
Number of fine mesh iterations for the inviscid flow	200
Subsonic flow relaxation parameter	0.7
Artificial viscosity parameter	0.800
Partially conservative parameter	0.25
Viscous relaxation parameter for coarse mesh	0.15
No. of inviscid flow iterations between each viscous update in coarse mesh	5
Viscous relaxation factor for fine mesh	0.075
No. of inviscid flow iterations between each viscous update in fine mesh	5
Increment in non-dimensional momentum thickness at XTU	0
Increment in non-dimensional momentum thickness at XTL	0

After running the programme, the correspond results form is shown below in Table 5-4. In VGK two different approaches are employed for calculating the aerofoil drag coefficient. These are the ‘near-field’ approach and the 'far-field' approach. In principle, the two approaches should lead to equal values for the overall drag coefficient. In this thesis, the near-field approach is chosen. In this approach the overall drag coefficient (which includes any wave drag) is evaluated by adding the contributions to the streamwise force from the surface pressures and the surface shear stresses (skin friction), thus CD=CDP+CDF.

Table 5-4 VGK calculation results

Freestream mach number	0.8
Incidence	0
Aerofoil lift coefficient	-0.00066
Pitching moment coefficient	0.00014
Contribution to Cd determined from integration of surface pressures CDP	0.00503
Contribution to Cd determined from integration of surface shear stresses CDF	0.00323
Viscous drag coefficient	0.00416

Use ESDU pac W0315 which is associated software related to reference [29] to calculate the aerodynamic characteristics of a two-dimensional single-element aerofoil in a subsonic free stream. Table 5-5 illustrates the results from this VGK method. As the aircraft is in the cruise flight, the aerodynamic characteristics like cl and cm may be linear.

Table 5-5 Aerodynamic coefficient of different AOA

	-3	-2	-1	0	1	2	3
cl	-0.5670	-0.3785	-0.1890	-0.0007	0.1877	0.3770	0.5655
cm	0.0124	0.0014	0.0004	0.0001	-0.0001	-0.0011	-0.0120
cdp	0.0239	0.0116	0.0062	0.0051	0.0062	0.0116	0.0238
cdf	0.0033	0.0034	0.0035	0.0035	0.0035	0.0034	0.0033
cd	0.0271	0.0150	0.0097	0.0086	0.0097	0.0149	0.0270

Figures 5-2, 5-3 and 5-4 show the relationship of aerodynamic coefficient with different AOA after using Excel to do the interpolation.

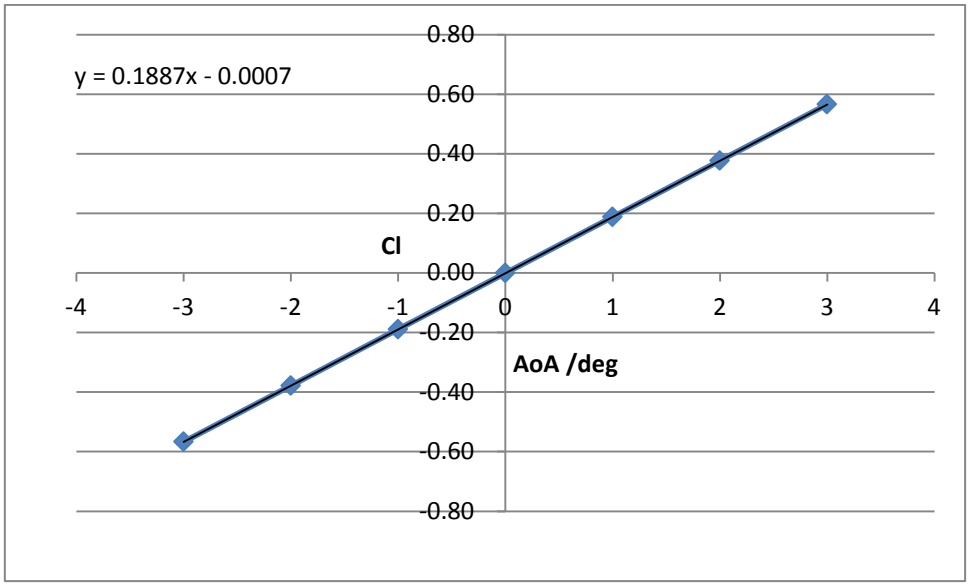

Figure 5-2 Cl of RC-SC2

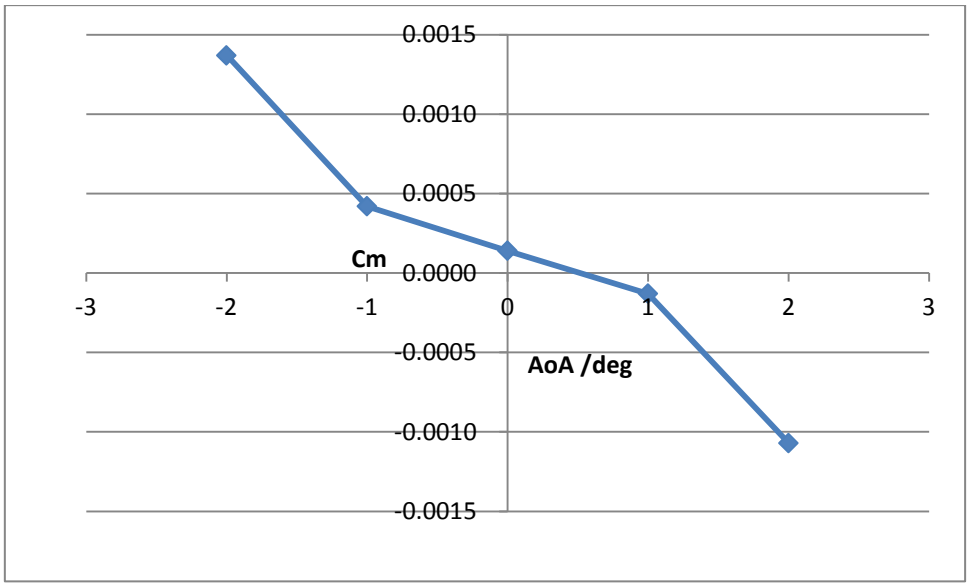

Figure 5-3 Cm of RC-SC2

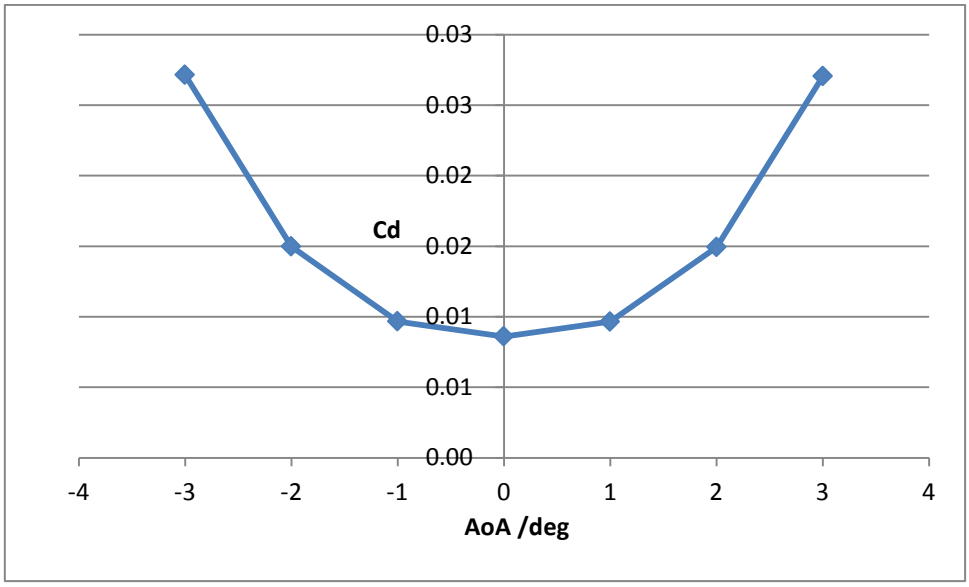

Figure 5-4 Cd of RC-SC2

B. Initiate angle of attack for level flight condition

The airfoil of inner wing is modified NACA Symmetrical Supercritical. In order to increase internal capacity, the thickness ratio has to be enlarged to 16%. The shape of modified airfoil is shown below in Figure 5-5.

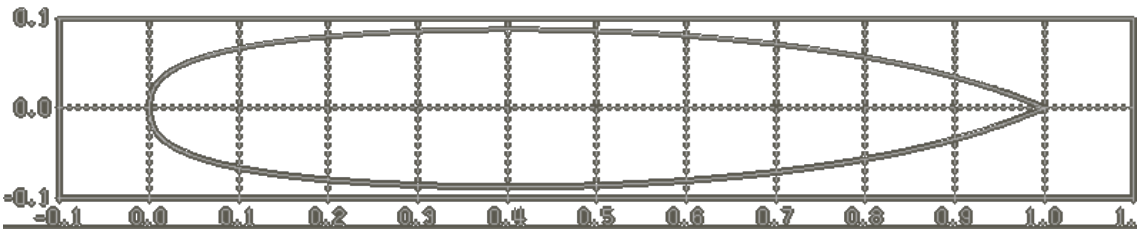

Figure 5-5 Geometry of inner wing

The general lift formula is

$$L = \frac{1}{2}\rho V^2 C_L S = \frac{1}{2}\rho V^2 (C_{Li} S_i + C_{Lo} S_o) \quad \textbf{(5-3)}$$

In the level flight condition, C_L is linear with the angle of attack. Figure 5-6 shows the lift coefficient of the inner wing.

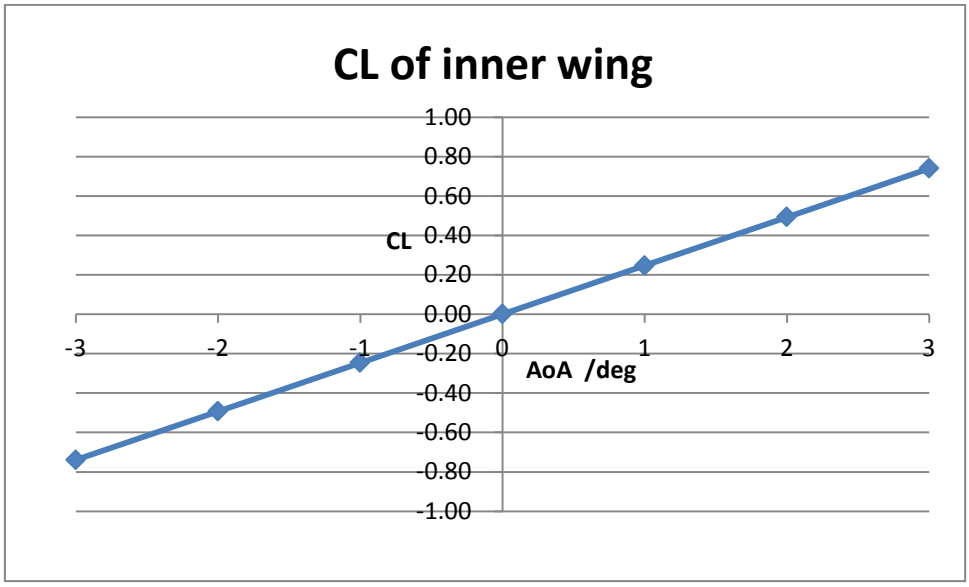

Figure 5-6 Lift coefficient of inner wing

In a steady flight condition, the lift generates by the inner wing and outer wing should be equal to the maximum takeoff weight of the aircraft:

$$\mathrm{L} = \mathrm{M_{to}g} \tag{5-4}$$

where, $\mathrm{M_{to}} = 176454\ \mathrm{kg}$,$a_{\mathrm{wo}} = 13.18/\mathrm{rad}$, $a_{\mathrm{wi}} = 10.89/\mathrm{rad}$

After calculation, the initiate angle of attack is 1 degree.

C. Aerodynamic characteristics for rolling effectiveness analyse

Use ESDU-01033 [30] to calculate aerodynamic characteristics of an aerofoil fitted with simple hinged flaps in subsonic airflow.

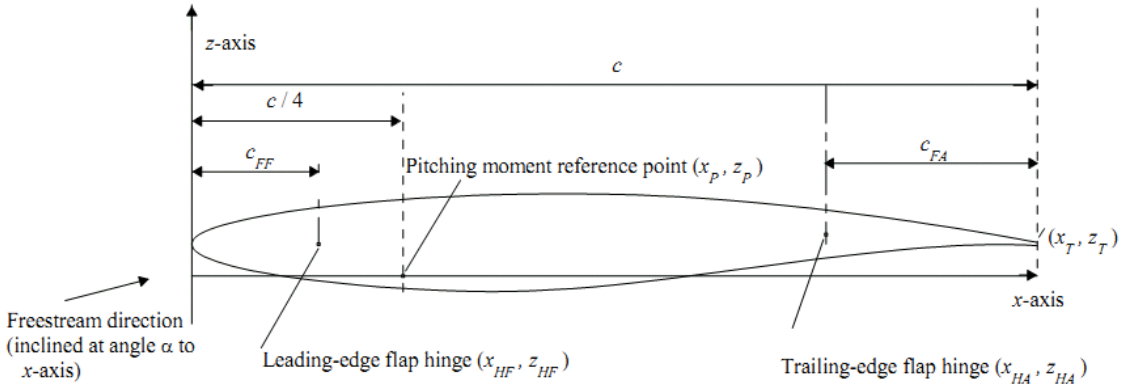

Figure 5-7 Airfoil with simple hinged flaps [30]

At first, use the program ADFLAP, which inputs the coordinates of the basic aerofoil, the flap hinge coordinates and the flap deflection angles to generate the new airfoil shape after the deflection. Secondly, ran the programme VGKCON to produce files in preparation for the program VGKSF, with the input data (similar to ESDU0315) as the airfoil geometry, Mach number, viscous relevant values and so on. Then ran the program VGKSF, get the results such as pressure distributions, surface grid coordinates and force and moment coefficients.

Calculate different deflections for different angle of attack. Then use the linearised interpolation method to get the relationship between aerodynamic characteristics and deflections of flaps and the angle of attack of the airfoil. Some results are shown in Table 5-6.

Table 5-6 Aerodynamic coefficient of different AOA and different flap angles

		b=-5	b=-2.5	b=0	b=2.5	b=5
a=0.6	cl	-0.49740	-0.19950	0.11011	0.41888	0.65232
	cm	0.10517	0.05131	-0.00053	-0.05156	-0.10799
a=0.4	cl	-0.52579	-0.22900	0.08073	0.38971	0.61156
	cm	0.10506	0.05146	-0.00045	-0.05110	-0.10122
a=0.3	cl	-0.55577	-0.25883	0.05098	0.36069	0.60406
	cm	0.10591	0.05170	-0.00027	-0.05102	-0.10332
a=-0.2	cl	-0.64838	-0.35855	-0.04872	0.26101	0.53511
	cm	0.10878	0.05135	0.00052	-0.05144	-0.10411

5.4 Conclusion

Based on the results from VGK method, using Excel to do the interpolation, the equation linking Cl and both the flap deflection and the angle of attack found is

$$Cl=0.19\alpha +0.123\beta \quad \textbf{(5-5)}$$

where α is the angle of attack of airfoil, β is the deflection of flap, and both unit is degree.

The equation linking Cm and both the flap deflection and the angle of attack found is

$$Cm=-0.000612\alpha-0.02\beta \quad \textbf{(5-6)}$$

The equation linking Cd and the angle of attack found is

$$Cd = 0.0021(\alpha)^2 - 1E\text{-}05\alpha+ 0.0075 \quad \textbf{(5-7)}$$

6 Development of deformation model

6.1 Introduction

Based on the loads model and aerodynamic loads, effect of wing flexibility on lift distribution is investigated. The deflection of flexible aircraft structure under aerodynamic loads is calculated, where the forces and moments are considered to be independent of time.

6.2 Flexural axis and shear centre

Shear centre is the point in the cross-section where a shear load causes no twist and a torque causes no bending. Flexural axis is the locus of the shear centre of each section along the member [31].

In this thesis, to decouple the bending and twisting, the aerodynamic forces and inertia forces are moved to the flexural axis and cause some moments, so the forces cause only the bending and the moments cause the only twisting.

6.3 Calculate the forces and moments

The forces include inertial forces and aerodynamic forces. In order to decouple the bending and twisting deformation, forces are moved to the flexural axis. The movement creates moments M_G caused by inertial forces and moments M_L caused by aerodynamic forces and aerodynamic moments M_m.

The CG position at 32% and 35% of mean aerodynamic chord is chosen along with a position of aerodynamic forces at 25% of MAC and flexural axis at 35% of MAC.

The assumption that forces and moments to increase the angle of attack are in the positive direction is made. For twisting, the direction is easy to identify. For bending, making wing downward is positive (which will be explained in the effect of wing sweep angle part later). Table 6-1 shows the direction of forces and moments.

Table 6-1 Direction of forces and moments

Items	direction
G	positive
L	negative
M_G	negative
M_L	positive
M_m	positive

6.4 Effect of wing sweep angle

The leading edge sweep angle of the FW-11 is 39 degrees. As indicated in Figure 6-1, bending changes the angle of attack due to the sweep angle. As illustrated in the picture below, the node ib actually increases more than the node if. For example, when the wing is bending upward, node if and node ib are both moving upward, node ib moves a greater distance, so this bending lets the airfoil go downward and decreases the angle of attack. Furthermore, sweep angle also leads to the coupling of bending and twisting, because of the aero flexural axis have the angle with the x axis (aircraft heading direction).

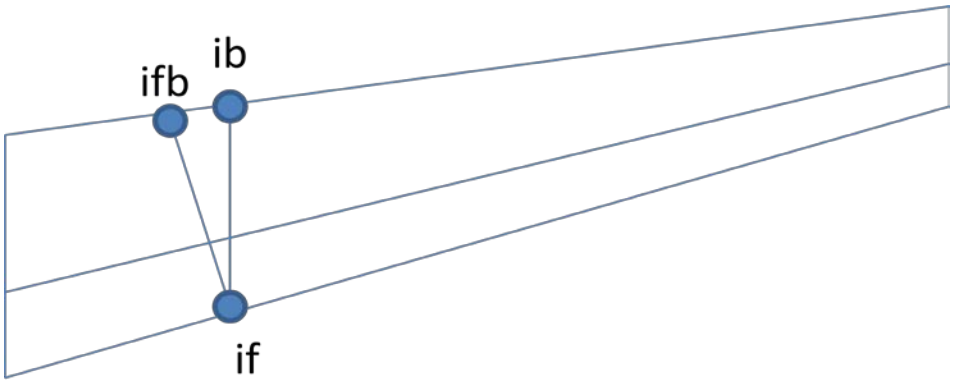

Figure 6-1 Wing sweep effect

6.5 Calculate bending and torsion moments to the flexural axis

As below, equation 6-1 and equation 6-2 explain how to make the moments from spanwise axis to flexural axis, to decouple the moments of bending and twisting.

$$M_b = M_{bs}\cos(\lambda) - M_{ts}\sin(\lambda) \tag{6-2}$$

$$M_t = M_{ts}\cos(\lambda) + M_{bs}\sin(\lambda) \tag{6-3}$$

In these two equations, M_{bs} and M_{ts} represent bending and torsion moment at spanwise axis respectively, and M_b and M_t represent bending and torsion moment at flexural axis . λ is the wing sweep angle of the flexural axis.

6.6 Calculate the initial deflection of the angle of attack

$$\theta = \int \frac{M_i}{GJ}\,dy \tag{6-4}$$

$$\Delta\,\mathrm{alfa}_t = \theta \tag{6-5}$$

Based on the elastic bending theory and the equation , $\Delta\,\mathrm{alfa}_t$ is the value which torsion moment changes.

$$\Delta\,w = w_{ib} - w_{if} = \iint \frac{M_{bib} - M_{bif}}{EI}\,dy \tag{6-6}$$

$$\Delta\,\mathrm{alfa}_b = \arctan(\Delta\,w/c) \tag{6-7}$$

As we can see from the two equations above , Δw is the bending deflection difference of one section, c is the length of the chord of that section, so $\Delta\,\mathrm{alfa}_b$ is the value which bending moment changes.

6.7 Principle of superposition

Assume that the system is linear elastic. If several loads effect at the same time, bending deflection and twisting angle of any section of the beam equals the sum of every load effecting separately.

$$\theta_i = \sum_{i=1}^{8} \int \frac{M_{ti}}{(GJ)_i}\,dy \tag{6-8}$$

$$\Delta\,wi = wi1 - wi2 = \sum_{i=1}^{8} \iint \frac{M_{bib} - M_{bif}}{(EI)_i}\,dy \tag{6-9}$$

$$\Delta\ \mathrm{alfa}_{\mathrm{ti}} = \theta_{\mathrm{i}} \tag{6-10}$$

$$\Delta\ \mathrm{alfa}_{\mathrm{bi}} = \arctan(\Delta\ \mathrm{w}_{\mathrm{i}}/\mathrm{c}_{\mathrm{i}}) \tag{6-11}$$

According to this principle, and apply the four equations above, the change in angle of attack caused by several different bending and torsion moments can be calculated.

With the strip method, the following equation can calculate the initial changing of angle of attack for each section.

$$\Delta\ \mathrm{alfa}_{\mathrm{i}} = \mathrm{alfa0}_{\mathrm{i}} + \Delta\ \mathrm{alfa}_{\mathrm{ti}} + \Delta\ \mathrm{alfa}_{\mathrm{bi}} \tag{6-12}$$

6.8 Interaction calculation

Put the beam model, initial flight condition and loads, aerodynamic data and structure data into MATLAB code. Then repeat the method from section 6.3 to section 6.7, to do the iteration calculation (repeating to calculate equation 6-12 for 100 times) with the interaction between aerodynamic and elastic forces. After that, the results are in table 6-2 and table 6-3 below for different inertia data. As the maximum error is less than 1%, so the aircraft can be considered achieving the equilibrium condition at this point.

Because the effect on the lift is the main concern of this case, the static aeroelastic deformation is presented by the angle of attack of different section of the outer wing as shown in Tables 6-2 and 6-3 .

Table 6-2 Deformation of each section of outer wing (CG=32% MAC)

CG=32% MAC	t=100	t=99	error
alfa1	0.01512	0.01511	0.093%
alfa2	0.01882	0.01877	0.303%
alfa3	0.00331	0.00330	0.335%
alfa4	-0.00189	-0.00188	0.850%
alfa5	-0.00386	-0.00387	-0.321%
alfa6	-0.00848	-0.00845	0.296%
alfa7	0.00754	0.00753	0.085%
alfa8	0.11114	0.11073	0.369%

Table 6-3 Deformation of each section of outer wing (CG=35% MAC)

CG=35% MAC	t=100	t=99	error
alfa1	0.01693	0.01690	0.136%
alfa2	0.01994	0.01988	0.306%
alfa3	0.00543	0.00548	-0.828%
alfa4	0.00042	0.00042	0.359%
alfa5	-0.00136	-0.00137	-0.772%
alfa6	-0.00555	-0.00551	0.753%
alfa7	0.00942	0.00949	-0.757%
alfa8	0.10030	0.09987	0.432%

6.9 Effect of wing flexibility on some lift parameters of the outer wing

6.9.1 Introduction

The investigation into effect of wing flexibility on some lift parameters is focused on the cruise flight condition. While the fuel in the outboard tank consumed, the location of weight in the outer wing has changed which definitely influences the deformation of the wing, so CG has to be considered. In order to find more ways to reduce the negative loss of the lift due to the flexible wing, more factors are investigated like the location of the lift and location of the flexural related to this phenomenon.

6.9.2 CG on the effect

The lift distribution of rigid and flexible wing with different CG is shown in Figure 6-2, which y axis is the distance ratio (the length from the root of the wing to the whole length of the wing). Figures 6-3 and 6-4 have the same y axis.

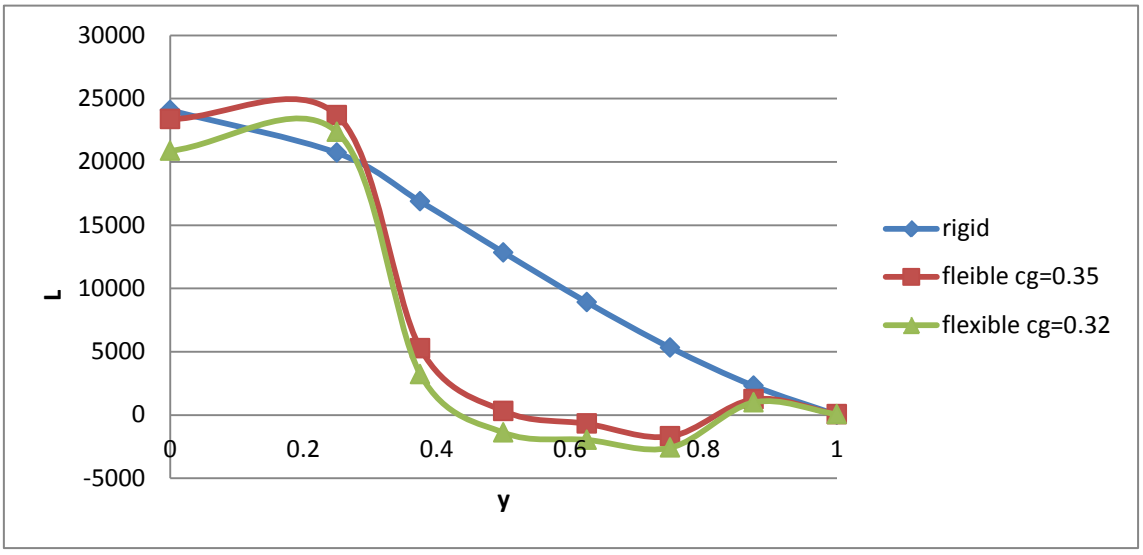

Figure 6-2 Lift distribution of rigid and flexible wing

Compared with the rigid one, the lift has been increased slightly near the root of the wing. At the point x=0.3, it begins to reduce fiercely to zero at x=0.4. Between x=0.4 and x=0.8, the lift becomes negative. After x=0.8, the lift rises up a little ,but still smaller than the rigid one. Compared the two lift curves of

flexible wing, it can be seen the lift distribution decreases slightly when the CG moves forward.

As can be seen from Table 6-4, lift is lost due to the flexibility of the wing. The flexibility of wing gives a negative influence on the lift. It reduces 34.1% when CG is at 35% MAC and 45.6% when CG is at 32% MAC. For the absolute value of lift loss, it is more significant when the outer wing fuel is consumed.

Table 6-4 Loss of lift and lift to weight ratio(CG factor)

<table>
<tr><th></th><th>Total Lift</th><th>Loss of lift</th><th colspan="2">Weight of total aircraft</th><th colspan="2">Loss of lift to weight(whole aircraft) ratio</th></tr>
<tr><td>Flexible wing (CG at 35%)</td><td>60026 N</td><td>30972 N (34.1%)</td><td colspan="2">1730141 N</td><td colspan="2">1.79%</td></tr>
<tr><td rowspan="2">Flexible wing (CG at 32%)</td><td rowspan="2">49441 N</td><td rowspan="2">41555 N (45.6%)</td><td>with inner wing fuel</td><td>without inner wing fuel</td><td>with inner wing fuel</td><td>without inner wing fuel</td></tr>
<tr><td>1696682 N</td><td>1016358 N</td><td>2.5%</td><td>4%</td></tr>
<tr><td>Rigid wing</td><td>51600 N</td><td colspan="4"></td></tr>
</table>

Considered the influence of the loss of lift for the whole aircraft, the lift to the weight (for the aircraft) ratio may be another important parameter to estimate the effect of flexible wing.

With the reference to Table 6-4, the loss of lift to weight ratio increases from 1.79% (with inner wing fuel)to 2.5% as the CG move forward. If the inner wing fuel is also burnt, the loss of lift ratio continues grows to 4%. It is clear that the effect of flexible wing on the loss of lift to weight ratio becomes larger when the aircraft continues the cruise flight with the fuel consumption.

The influence of flexible wing on the loss of lift to weight ratio rises as the fuel burnt and it also means the CG of outer wing is more forward, the bigger loss of lift to weight ration.

Moving CG of outer wing more backward by readjusting the layout of the outer board wing is one way to weaken the effect of wing flexibility on the lift to weight ratio loss.

But, move the CG backward is not a recommend method for it reducing the static margin of the aircraft, especially for the flying configuration which has little or negative static margin.

6.9.3 Location of lift and location of flexural axis on the effect

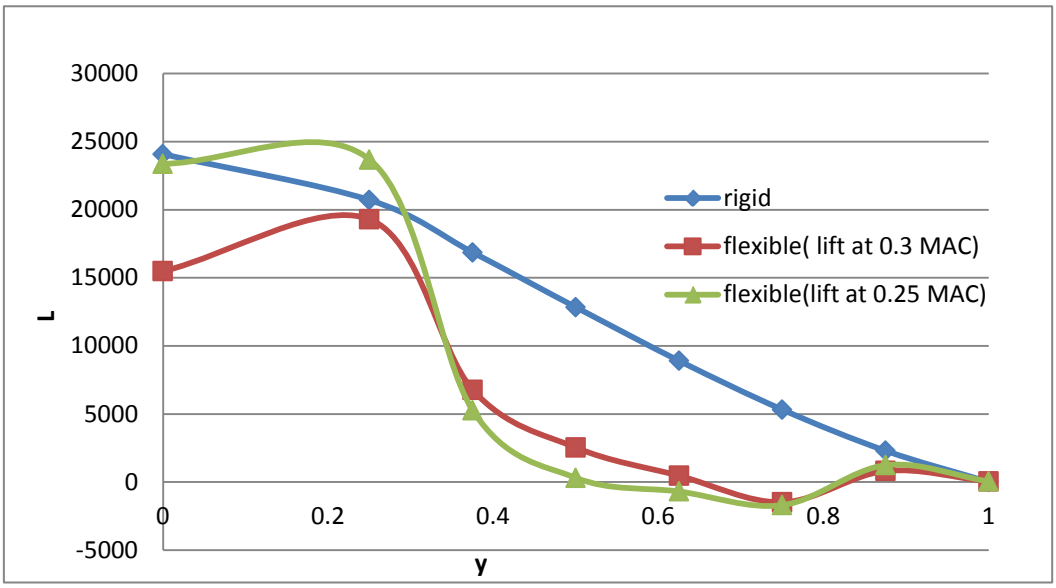

Figure 6-3 Lift distribution of rigid and flexible wing(Location of lift)

Figure 6-3 shows lift distribution of different location of lift. Unlike Figure 6-2, as the lift move backward, the lift near the root becomes smaller while the lift near the tip becomes larger.

Table 6-5 Loss of lift and lift to weight ratio(Location of lift)

	Total Lift	Loss of lift	Weight of aircraft	Loss of lift to weight(whole aircraft) ratio
Flexible wing (Lift at 25%)	60026 N	30972 N (34.1%)	1730141 N	1.79%
Flexible wing (Lift at 30%)	51600 N	39396 N (43.3%)	1696682 N	2.3%
Rigid wing	90996			

	N

With the reference to Table 6-5, the total lift becomes smaller as the lift moves backward and also the loss of lift to weight ratio turns into a bigger value. As the lift moves backward, it adds the effect of wing flexibility on the lift and gives more negative influence.

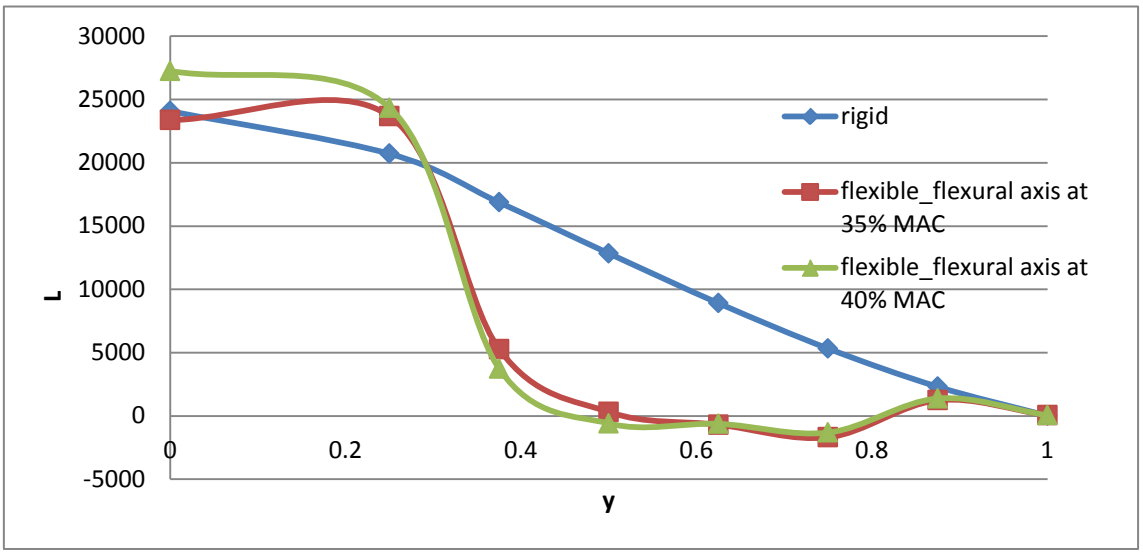

Figure 6-4 Lift distribution of rigid and flexible wing (Location of flexural axis)

It is shown lift distribution for different location of flexural axis in Figure 6-4, similar with Figure 6-3. As the flexural axis move backward, the lift before x=0.4 becomes larger and after x=0.4 remains nearly the same.

From Table 6-6, as flexural axis also moves back 5%, the total lift has increased from 60026 to 62709, but not significant as moving the lift.

Table 6-6 Loss of lift and lift to weight ratio (Location of flexural axis)

	Total Lift	Loss of lift	Weight of aircraft	Loss of lift to weight(whole aircraft) ratio
Flexible wing (flexural axis at 35%)	60026 N	30972 N (34.1%)	1730141 N	1.79%
Flexible wing (flexural axis at 40%	62709 N	28287 N (31.1%)	1696682 N	1.67%

Rigid wing	90996 N

6.9.4 Conclusion

It is clear that the effect of wing flexibility has negative influence on the lift. Compared with the rigid aircraft, the total lift of outer wing has been decreased 34.1% when CG is at 35% MAC and 45.6% when CG is at 32% MAC. The loss of lift to weight ratio increases from 1.79% to 2.5% as the CG move from 35% to 32%.

The reduction of lift may be more significant than the conventional aircraft. Author thinks the main reason is that the flying wing configuration has smaller angle of attack in the steady level flight due to its large lifting surface. Expressed as percentage，the deformation is more noticeable. Because of the flying wing configuration, the inner wing generates the majority part of the lift which is much less flexible (considered rigid in this thesis). Using the elevator may balance the loss of lift and trim the aircraft in a new steady situation.

Move CG backward, move lift forward and move flexural axis backward can reduce this negative influence. Because they all decrease the torsion moment, which weaken the deformation of the wing.

7 Evaluation on some effects of aeroelasticity on the rolling effectiveness

7.1 Introduction

Control surfaces are used to manoeuvre the aircraft by changing the pressure distribution and this lead to change the lift. In this section, the effect that aeroelastic deformation on the aerodynamic influence, to be more specific, the effectiveness of the aileron in comparison to the rigid one is considered. It is illustrated that as the speed increases, the effectiveness reduces until at certain critical speed which is named reversal speed. At this speed, there is no response to application of the aileron. As the speed is greater than the reversal speed, the action of the aileron reverses, which is known as control reversal.

In this thesis, in order to make model simple and clear, and avoid calculating a large number of flexible derivatives, the simplified pure roll case is considered. The coupling effects of yaw and sideslip are neglected.

If the dihedral effect is considered, the roll moment due to sideslip is negative since this will tend to oppose the roll movement. This effect will reduce the effect of aeroelasticity on the roll effectiveness. According to the equations from reference 18, L_p/L_v is more than 10 times (assume the dihedral angle is 1 degree). L_v may be ignored for the calculation in this simplified roll case.

This is another case that is independence with the effect of wing flexibility on lift distribution. The wing twist due to the flexible deformation at y (along the spanwise direction) is $\frac{y}{s} q_e$.

7.2 Lateral derivatives

7.2.1 Lateral derivatives for rigid aircraft

7.2.1.1 Rolling moment derivative due to the roll rate

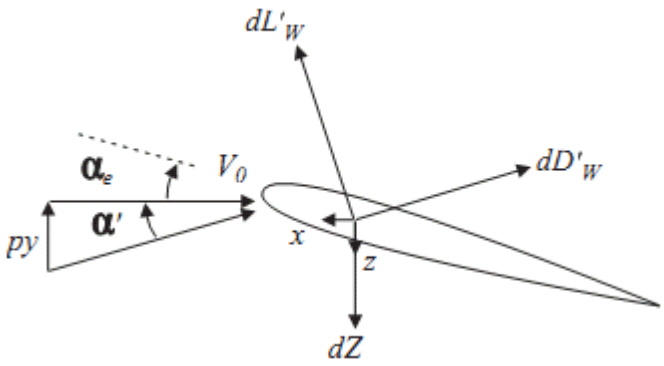

Figure 7-1 Airfoil of the wing in rolling flight-perturbed state

As FW-11 is the flying wing configuration, this damping derivative arises only from the wing. The aircraft in steady flight is at velocity $V_0 = 0.8$， $Ma = 240\ m/s$ and the trimmed angle of attack is $\alpha_e = 1°$. When the aircraft experiences a perturbation in the roll rate p, then there is an effective change of angle of attack on each wing strip dy, as shown in Figure 7-1 (a strip on the starboard wing). The effective increase in angle of attack for the elemental section at position y is [18]

$$\alpha' \cong \tan(\alpha') = \frac{py}{V_0} \tag{7-1}$$

where $py \ll V_0$.

The strip lift and drag in the perturbed state are normal to and along the perturbed velocity vector, so

$$dL'_w = \frac{1}{2}\rho v_0^2 c\alpha_W \left(\alpha_e + \frac{py}{v_0}\right) dy \tag{7-2}$$

$$dD'_w = \frac{1}{2}\rho v_0^2 c C_D dy \tag{7-3}$$

Referring to Figure 7-1, the normal force in the wind axes direction, corresponding to the perturbed state, is given by

$$dz = -dL'_w \cos(\alpha') - dD'_w \sin(\alpha') \approx -dL'_w - dD'_w \alpha' \quad \textbf{(7-4)}$$

The elemental contribution to the rolling moment is

$$dL = ydZ = (-dL'_w - dD'_w \alpha')y = -\frac{1}{2}\rho v_0^2 \left[a_W \alpha_e + (a_W + C_D)\frac{py}{v_0}\right] cydy \quad \textbf{(7-5)}$$

When the equivalent expression is obtained for a strip on the port side and two rolling moment contributions added, the terms involving the trim angle of attack α_e cancel out as they cause no net roll effect. The total rolling moment may then be written as

$$L = -2\int_0^s \frac{1}{2}\rho v_0^2 c\,(a_W + C_D)\frac{py}{v_0} ydy \quad \textbf{(7-6)}$$

Consider equation $L = L_p * p$, and evaluate the integral, so the aerodynamic rolling moment due to the roll rate derivative

$$L_p = -\frac{1}{2}\rho v_0^2 [\frac{S_w(a_w + C_D)s^2}{3}] \quad \textbf{(7-7)}$$

7.2.1.2 Rolling moment derivative due to aileron

Figure 7-2 Layout of the control surfaces of the outer wing

The layout of the aileron is shown in Figure 7-2 and the position of it is approximately at section 3 and section 4 of the outer wing. The rolling moment due to applying the aileron through a perturbation in ξ needs to be determined. The life force perturbation developed on an airfoil section on the starboard wing due to control rotation is

$$\mathrm{d}L'_{\mathrm{w}} = \frac{1}{2}\rho v_0^2 c a_{\mathrm{c}} \xi \mathrm{d}y \tag{7-8}$$

where ξ is the aileron angle (positive trailing edge down) and α_{c} is the sectional lift coefficient per control angle. The normal force perturbation is then given by $\mathrm{d}Z = -\mathrm{d}L_{\mathrm{w}}$, since the wind axes are not perturbed. The rolling moment from each wing is the same and by integration, the total rolling moment is given by

$$L = 2\int_{y_2}^{y_4} \frac{1}{2}\rho v_0^2 c a_{\mathrm{c}} \xi y \mathrm{d}y \tag{7-9}$$

After evaluating the integral, the rolling moment due to aileron derivatives is

$$L_\xi = \frac{1}{2}\rho v_0^2 \left(\frac{S_{\mathrm{aileron}} a_{\mathrm{c}} s}{2}\right) \tag{7-10}$$

7.2.2 Lateral derivatives for flexible aircraft

$$L = L_{\mathrm{p}} p + L_\xi \xi + L_{\mathrm{e}} q_{\mathrm{e}} \tag{7-11}$$

$$Q_{\mathrm{ext}} = Q_{\mathrm{p}} p + Q_\xi \xi + Q_{\mathrm{e}} q_{\mathrm{e}} \tag{7-12}$$

Now consider the flexible aircraft experiencing an aileron input ξ (trailing edge upwards/downwards on the starboard/port wings). There is a perturbed lift contribution due to the upwards velocity of the air stream relative to the wing and also due to the angle of twist; the rate of twist deformation with time may be assumed to cause no net aerodynamic effect if unsteady effects are ignored The perturbed lift $\mathrm{d}L_{\mathrm{A}}$ due to aileron is shown in its positive sense, though it is negative for aileron up. Thus the perturbed lift force on the starboard wing strip is given by

$$dL_{W+A} = dL_w + dL_A = \frac{1}{2}\rho v_0^2 \left\{ a_W \left[\alpha_e + \frac{py}{v_0} + \gamma_e(y) q_e \right] - a_c \xi \right\} c dy \quad \textbf{(7-13)}$$

where the perturbed lift contribution due to flexibility is used to determine the unknown elastic derivatives. The drag contribution and any effect of perturbed axes has been neglected for flexible derivatives. The contribution to rolling moment of the flexible deformation term in this equation is given by integration, so

$$L_e = -2 \int_0^s \frac{1}{2}\rho v_0^2 a_W \gamma_e(y) y c dy \quad \textbf{(7-14)}$$

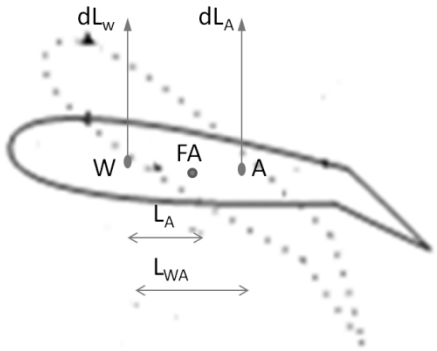

Figure 7-3 Wing section for flexible twist deformation

To determine the derivatives associated with the perturbed flexible mode deformation, the incremental work done by the aerodynamic lift forces moving through the incremental deformation of the mode must be obtained. Now it is assumed that the lift on the wing (due to the roll rate and twist) acts at the quarter chord (W, for wing aerodynamic centre) and that the additional lift due to the aileron deflection acts at a distance L_{WA} behind the aerodynamic centre (A) which is at 40% of the chord. Because the flexural axis (FA) lies a distance L_A behind the aerodynamic centre, the respective incremental displacements (upwards positive on the starboard wing) are given by

$$\delta z_w = L_A \gamma_e(y) \delta q_e \quad \textbf{(7-15)}$$

$$\delta z_A = -(L_{WA} - L_A)\gamma_e(y)\,\delta q_e \tag{7-16}$$

and the incremental work done term due to flexible deformation is

$$\delta W_e = 2\int_0^s dL_w\,\delta z_w + 2\int_0^s dL_A\,\delta z_A \tag{7-17}$$

The generalized/modal force is then given by

$$Q = \frac{\partial(\delta W_e)}{\partial(\delta q_e)} = Q_p p + Q_\xi \xi + Q_e q_e \tag{7-18}$$

and, by inspection, it may be shown that the flexible derivatives are

$$Q_p = 2\int_0^s \frac{1}{2}\rho v_0^2 a_W \left[\alpha_e + \frac{py}{v_0}\right] c\, L_A \gamma_e(y)dy \tag{7-19}$$

$$Q_e = 2\int_0^s \frac{1}{2}\rho v_0^2 a_W \gamma_e^2(y) q_e\, cL_A dy \tag{7-20}$$

$$Q_\xi = 2\int_0^s \frac{1}{2}\rho v_0^2 a_c \xi (L_{WA} - L_A)\gamma_e(y)dy \tag{7-21}$$

7.2.3 Value of derivatives

With the reference of Equation 7-7,7-9,7-13,7-18,7-19 and 7-20, the value of derivatives for rolling of both rigid and flexible aircraft are calculated and the results presented in Table 7-1.

Table 7-1 Value of the derivatives

L_p	-1809200
L_ξ	7404100
L_e	-27110000
Q_p	45184
Q_ξ	740410

Q_e	222590

7.2.4 The influence of the location of the lift on variations of the derivatives

From the equations shown in section 7.2.1, the location of the additional lift due to the aileron deflection (L_{WA}, from Figure 7-3) influences the derivative Q_ξ and the location of the aerodynamic centre (L_A, from Figure 7-3) influences the derivatives Q_p, Q_ξ and Q_e. Some results about this influence of these derivatives to variations in the location of lift are shown in Table 7-2. As L_{WA} and L_A become smaller, which means the location of lift moves forward, Q_ξ is the most sensitive derivative.

Table 7-2 Influence on variations of the derivatives

	$L_A = 0.1c$ $L_{WA} = 0.15c$	$L_A = 0.1c$ $L_{WA} = 0.13c$	error
Q_ξ	23138	13883	40.00%
	$L_A = 0.1c$ $L_{WA} = 0.15c$	$L_A = 0.08c$ $L_{WA} = 0.13c$	
Q_p	45184	42925	5.00%
Q_ξ	23138	42925	-40.00%
Q_e	677760	32393	12.50%

7.3 Rolling effectiveness of rigid aircraft

Firstly, the transient roll rate response is calculated. Then the steady-state roll rate per aileron is estimated.

$$I_x\dot{p} - L_p p = L_\xi \xi \qquad \textbf{(7-22)}$$

For a general aileron input, the equation of the transient roll rate response may be solved in the time domain. Given a step aileron angle $\xi_0 = 2°$, the response may be shown to be

$$p(t) = -\frac{L_\xi}{L_p}\left[1 - \exp\left(\frac{L_p}{I_x}t\right)\right]\xi_0 \quad \textbf{(7-23)}$$

During the level flight, as the consumption of the fuel, I_x is reduced. For FW-11 is long endurance aircraft, the initial state and final state of the cruise condition, so I_x changes significantly. These two states are considered in this case as shown in table 7-3.

Table 7-3 Value of the moment of inertia in roll

	With full fuel	Without fuel
I_x of $FW-11(kg*m\text{^}2)$	10391139	3430236

Figures 7-4 and 7-5 show transient roll rate response of the rigid aircraft, with fuel and without fuel. As can be seen from the two figures, roll rate takes much longer time to become steady when I_x is larger.

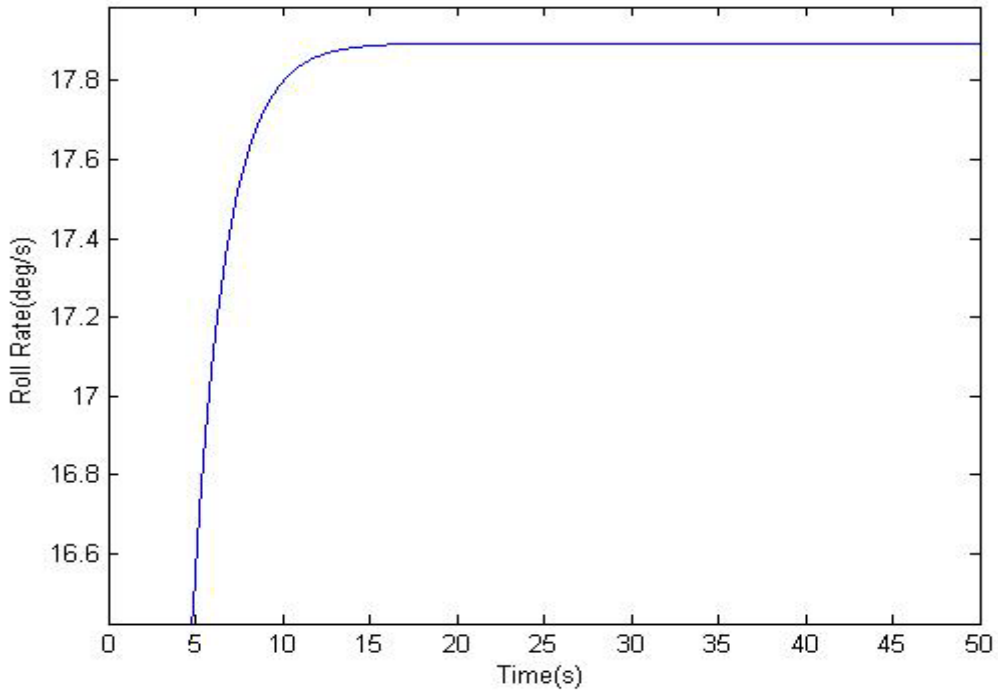

Figure 7-4 Transient roll rate response of rigid aircraft(without fuel)

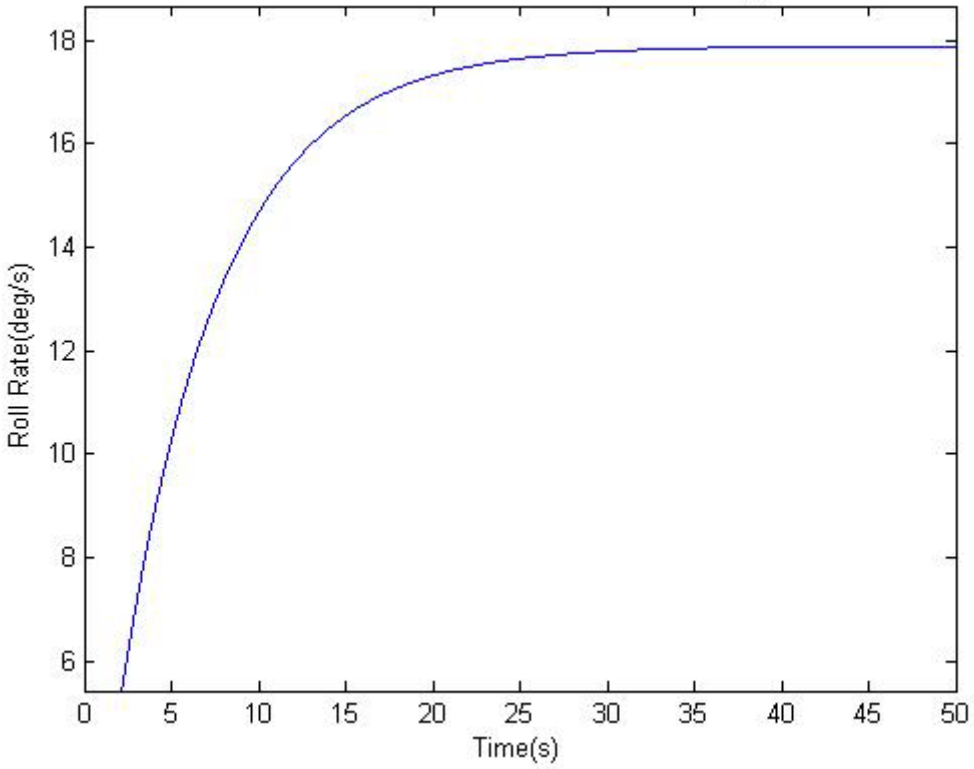

Figure 7-5 Transient roll rate response of rigid aircraft(with fuel)

The aircraft behaves like a simple lag with a decaying exponent dependent upon the roll damping derivative. The steady-state roll rate following a step aileron input is found by setting the roll acceleration $\dot{p}$ to zero.

The transfer function between the roll rate and aileron angle may be found by transforming the differential equation of motion (7-21) into Laplace form , so

$$\frac{p}{\xi}(s) = \frac{L_\xi}{I_x s - L_p} \tag{7-24}$$

This function shows the variation with frequency of the gain and phase lag between the roll rate and an oscillatory aileron input. The denominator, when set to zero, defines the characteristic equation of the system

$$I_x s - L_p = 0 \tag{7-25}$$

The steady-state roll rate per aileron angle is found from the value of the transfer function at zero frequency, so

$$\frac{p}{\xi}(s) = -\frac{L_\xi}{L_p} = 5.52 \tag{7-26}$$

7.4 Rolling effectiveness of flexible aircraft

The transfer function relating roll rate to aileron angle may be found from Equations (3-14 & 3-15) in the Laplace domain:

$$\begin{bmatrix} I_x s - L_p & -L_e \\ -Q_p & m_e s^2 + c_e s + (k_e - Q_e) \end{bmatrix} \begin{bmatrix} p(s) \\ q_e(s) \end{bmatrix} = \begin{bmatrix} L_\xi \\ Q_\xi \end{bmatrix} \xi(s) \tag{7-27}$$

This matrix equation may be solved to give the roll rate per aileron angle

$$\left(\frac{p}{\xi}(s)\right)_{\text{Elastic}} = \frac{s^2 L_\xi m_e + s L_\xi c_e + L_\xi (k_e - Q_e) + L_e Q_\xi}{D(s)} \tag{7-28}$$

Here the denominator polynomial D(s) is the determinant of the square matrix in Equation (7-23) such that

$$\begin{aligned} D(s) = s^3 (I_x m_e) + s^2 \left(I_x c_e - L_p m_e\right) + s\left[I_x (k_e - Q_e) - L_p c_e\right] \\ + \left[-L_p (k_e - Q_e) - L_e Q_p\right] \end{aligned} \tag{7-29}$$

Which, when set to zero, defines the characteristic (cubic) equation. The roots of this polynomial define the characteristic motions of the flexible aircraft in roll, namely a roll subsidence and an oscillatory flexible mode. The steady state roll rate per aileron deflection is given by the transfer function at zero frequency, namely,

$$\left(\frac{p}{\xi}\right)_{\text{Flexible}} = \frac{L_\xi (k_e - Q_e) + L_e Q_\xi}{-L_p (k_e - Q_e) - L_e Q_p} \tag{7-30}$$

The ratio of the flexible to rigid of the steady-state roll rate per aileron angle provides a measure of aileron effectiveness , i.e. how the aileron power is influenced by the flexible deformation, so

$$\delta_{\text{Aileron}=\frac{(p/\xi)_{\text{Flexible}}}{(p/\xi)_{\text{Rigid}}}} \quad \textbf{(7-31)}$$

Consider the behaviour of the aircraft having the 12Hz natural frequency and 4% damping mode, and flying at 240 m/s first. The aileron effectiveness with the change in velocity are shown in Figure7-6. Increasing the velocity would make the effects of flexibility more severe. It is clear that the effectiveness decreased with an increase in air speed and eventually becomes negative.

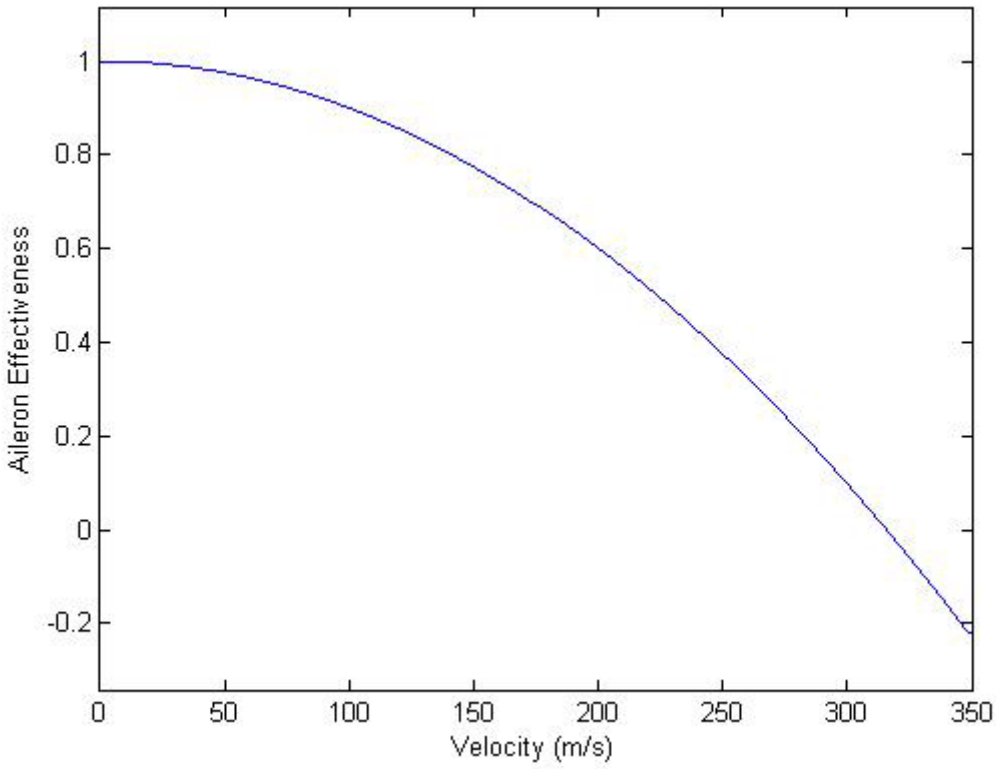

Figure 7-6 Aileron effectiveness with the change in velocity

In table 7-4, the variation in aileron reversal speed is shown for different torsional natural frequencies. At this speed, the rolling moment due to apply the ailerons is exactly balanced by the opposite rolling moment that generates due to the deformation of the wing. As the natural frequency decreases, the correspond reversal speed also reduces. In order to avoid control reversal, increase natural frequency is a feasible way.

Table 7-4 Reversal speed for different torsional natural frequencies

	6 Hz/ 4%	8 HZ/ 4%	12 Hz/ 4%
Reversal speed of aileron	161 m/s	215 m/s	322 m/s

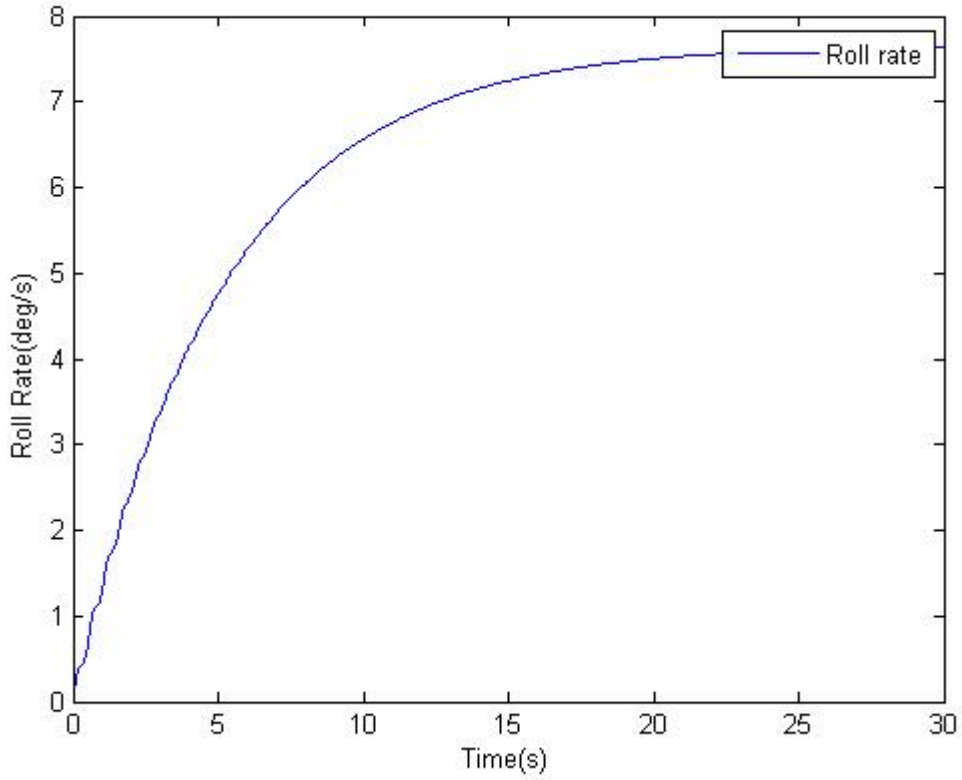

Figure 7-7 Transient roll rate response (12 HZ, with fuel)

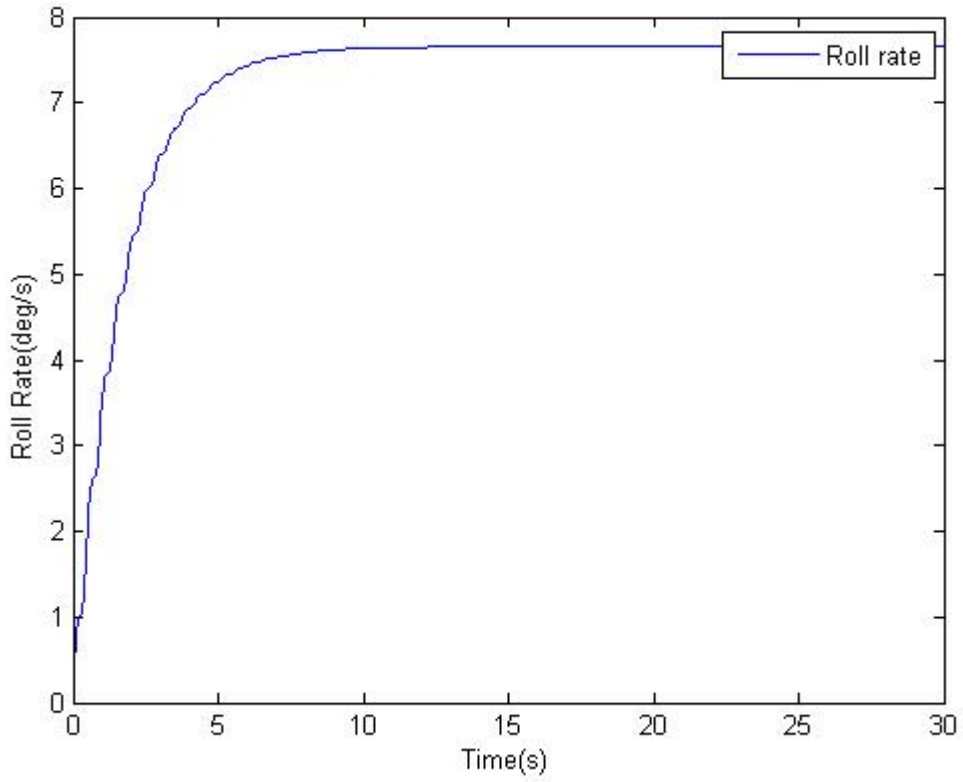

Figure 7-8 Transient roll rate response (12Hz without fuel)

Figure7-7 and Figure 7-8 show the response when the aileron rate ,when aileron applied 2 degrees, with fuel and without fuel respectively.

Table 7-5 Roll rate comparison

	Rigid aircraft		Flexible aircraft	
	With fuel	Without fuel	With fuel	Without fuel
Steady roll rate(deg/s)	17.8	17.8	7.7	7.7
Time to get steady(s)	35	15	26	12

As shown in table 7-5, inertial parameters, I_x and m_e , are changing as the fuel burnt, they influence the time of getting steady roll rate. It takes less time to get steady as I_x and m_e becoming smaller. It can be also found that these two inertial parameters do not change the final steady roll rate for both rigid aircraft and flexible aircraft. The steady roll rate of flexible aircraft is about 7.7 deg/s,

compared to the rigid aircraft value which is about 17.8 deg/s. The aileron effectiveness is 0.43, also can be seen from Figure 7-6. The reason to cause this phenomenon is that twist of the wing opposes the normal operation of the aileron.

Changing the torsional natural frequency from 12 Hz to 8 Hz, the reversal speed reduces from 316.09 m/s to 210.72 m/s and cause the control reversal. Transient roll rate response is shown in Figures 7-9 and 7-10.

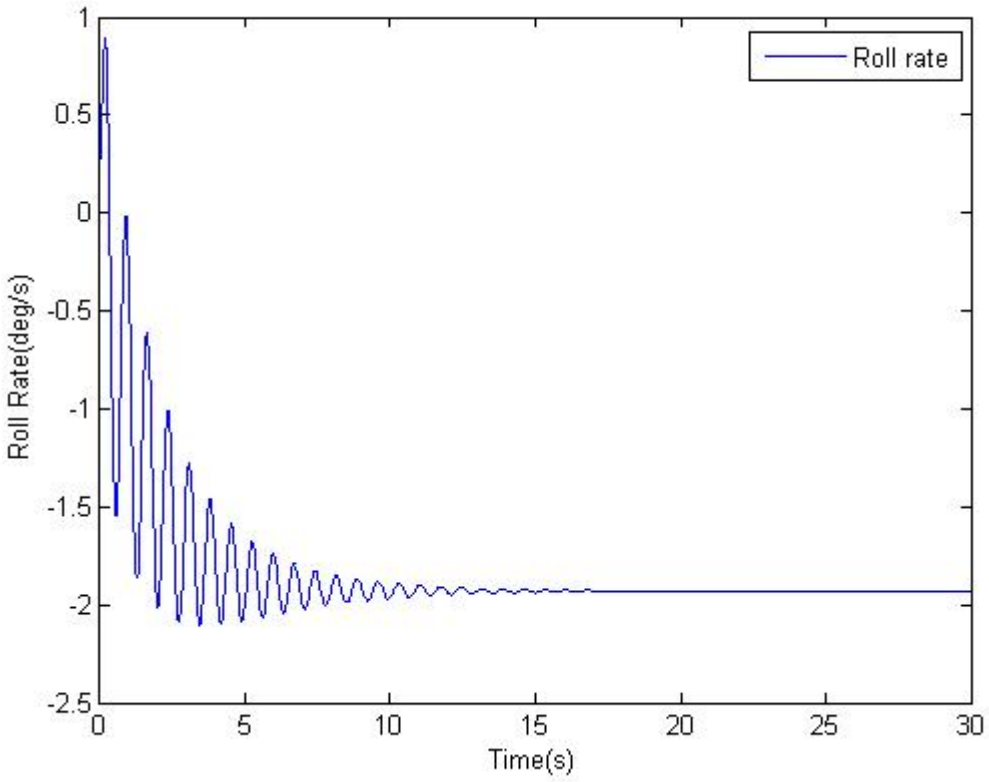

Figure 7-9 Transient roll rate response (8Hz without fuel)

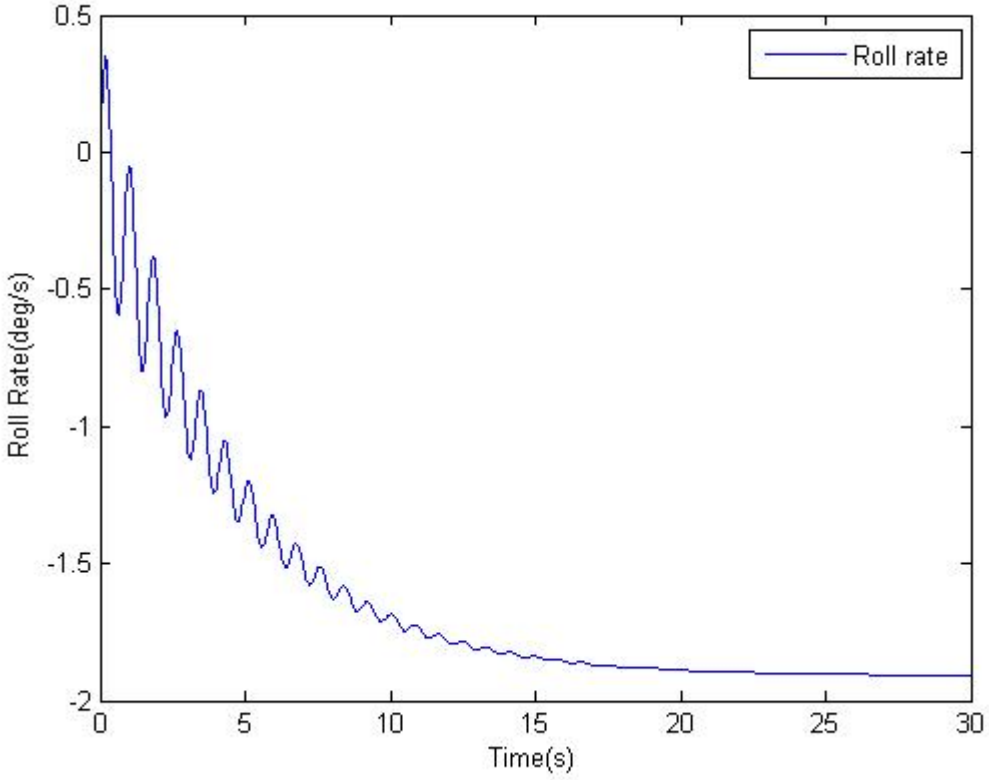

Figure 7-10 Transient roll rate response (8Hz with fuel)

As can be seen from the two figures above, the steady roll rate of flexible aircraft is about -1.8 deg/s, compared to the rigid aircraft value which is about 17.8 deg/s. The aileron effectiveness changes to -0.10. Also, from Figure7-7 to Figure7-10, the roll rate vibration at the beginning is more fierce when I_x and m_e are smaller.

It has been found that flexible wing leads to the loss of control effectiveness, even cause reversal when the structure natural frequency reduces.

8 Conclusions

In this research program, FW-11 is the investigation target aircraft. Consider the inner wing is rigid and the outer wing is flexible. Two cases are studied in the thesis.

One is to investigate the deformation of the wing and effect of wing flexibility on lift distribution in the level flight condition. In this case, it is the static aeroelastic analyse, so the forces are independent with time. It is clear that the effect of wing flexibility has negative influence on the lift. Compared with the rigid aircraft, the total lift of outer wing has been decreased 34.1% when CG is at 35% MAC and 45.6% when CG is at 32% MAC. The loss of lift to weight ratio increases from 1.79% to 2.5% as the CG move from 35% to 32%. The reduction of lift may be more significant than the conventional aircraft. One reason may be the flying wing configuration having smaller angle of attack in the steady level flight due to its large lifting surface. Expressed as percentage，the deformation is more noticeable. Because of the flying wing configuration, the inner wing generates the majority part of the lift which is much less flexible (considered rigid in this thesis). Using the elevator may balance the loss of lift and trim the aircraft in a new steady situation. After investigation, move CG backward, move lift forward and move flexural axis backward can reduce this negative influence. Because they all decrease the torsion moment which weaken the deformation of the wing.

The other case is to calculate the transient response and estimate the rolling effectiveness of flexible aircraft, and compared with the rigid aircraft's. It is quite clear that flexible wing leads to the loss of control effectiveness, even cause reversal for the specified torsion mode. Inertia parameters I_x and m_e are found to influence the time to get steady roll rate and level of the beginning vibration of rolling. The aileron effectiveness is 0.43 of the 12Hz /4% modal and -0.1 of 8Hz /4% modal. When the structure frequency reduces, the flexible effect can be more significant. Two ways are suggested to deal with this problem. One is to add the stiffness of the structure to increase the torsional natural frequency, and the other is to design the flight control system to suppress this interaction.

9 Future work

For future work, based on the method presented in this thesis, which includes the method for mass distribution calculation, stiffness calculation and aerodynamic calculation, the effects of wing flexibility on the other control surfaces can be estimated. To get a deeper understanding of the effects of wing flexibility on the full flight dynamics, both longitudinal and lateral-directional dynamics, need to be investigated.

When FW-11 comes to the preliminary design stage, more details about structure and control system are available. The method presented in this thesis can be modified to higher accuracy. Also, the results of this method can be used as reference data to optimize the structure and control system.

REFERENCES

1. Jian Wang, Final Presentation for AVIC GDP FW-11, Cranfield University, UK, 2011
2. A.L. Bolsunovsky, Flying wing- problems and decisions, Aircraft Design 4(2001) 193-219
3. Wood, R. M., & Bauer, S. S. Flying wings / flying fuselages, AIAA, 2001.
4. http://www.ctie.monash.edu.au/hargrave/northrop.html
5. http://www.as.northropgrumman.com/products/b2spirit
6. Dewey H. Hodges, Introduction to Structural Dynamics and Aeroelasticity, Cambridge University Press, 2002
7. Earl H. Dowell, A modern course in aeroelasticity, Kluwer Academic Publishers, 1995
8. Collar. A.R, The first fifty years of aeroelasticity, Aerospace, February, 12-20, 1978
9. Jan R Wright and Jonathan E Cooper, Introduction to Aircraft Aeroelasticity and Loads, John Wiley & Sons, Ltd., 2007
10. Lomax, T.L, Structure Loads Analysis for Commercial Transport Aircraft: Theory and Practice, AIAA Education Series, 1996
11. ESDU No. 96028, VGK method for two-dimensional aerofoil sections Part 1: principles and results. Engineering Science Data Unit International plc, 2004
12. Roland D.English, Some effects of aeroelasticity and sweepback on the rolling effectiveness and drag of A 1/11-scale model of the bell X-5 airplane wing at mach numbers from 0.6 to1.5, Langley Aeronautical Laboratory, 1956
13. Ludovic Bonnet, Design of a flexible composite wing trailing edge structure, MSc Report, Cranfield University,2005
14. Yan Yu, CFD simulations of a 3D composite wing with aero-elastic effects, MSc Report, Cranfield University,2010
15. Huizu, Dan, Mechanics of Materials, National Defense Industry Press, 1986
16. A. R. Amrane, “Flight dynamics model of a high-performance Sailplane”, M.Sc. Thesis, Cranfield University, 2005

17. Yates, E.C, Modified strip analysis method for predicting wing flutter at subsonic to hypersonic speeds, Journal of Aircraft,3(1), 25-9, 1966
18. Cooke, M. V, Flight dynamics principles, Elsevier Ltd., 2007
19. Haidong Huang，Geometric model of Final Presentation for AVIC GDP FW-11, Cranfield University, UK, 2011
20. D Howe, Blended wing body airframe mass prediction, Proceedings of the Institution of Mechanical Engineers Part G Journal of Aerospace Engineering, 01/01/2001
21. Cranfield University, Aircraft Mass Prediction, DAET 9317
22. Yuqing Qiao, Mass &CG part of Final Presentation for AVIC GDP FW-11, Cranfield University, UK, 2011.
23. S. Guo, User's guide for program boxmxesc.exe, 2004
24. Mark Drela and Harold Youngren, AVL version 3.26, MIT Aero & Astro Department, 2006
25. Mark Drela and Harold Youngren, Xfoil 6.9, MIT Aero & Astro Department, 2001
26. ESDU No. 96028, TVGK method for two-dimensional aerofoil sections Part 1: principles and results. Engineering Science Data Unit International plc, 2004
27. Faliang Wang, Aerodynamic part of Final Presentation for AVIC GDP FW-11, Cranfield University, UK, 2011.
28. http://www.digitalducth.com
29. ESDU No. 03015, Transonic data memorandum VGK method for two-dimensional aerofoil sections Part 7: VGK for Windows. Engineering Science Data Unit International plc, 2004
30. ESDU No. 01033, Transonic data memorandum VGK method for two-dimensional aerofoil sections Part 6: Aerofoil with simple hinged flaps. Engineering Science Data Unit International plc, 2001
31. Megson, T.H.G, Aircraft Structure for Engineering student, Arnold, 1999

APPENDICES

Appendix A Brief Introduction of GDP Work

A.1 Introduction

The conceptual design process is divided into two different stages. One is conceptual design for baseline aircraft which is the same requirements as the flying wing aircraft, in order to familiar with the whole process, and the other is conceptual design for flying wing which is target aircraft of GDP. In the first stage, the author is involved in the engine team and mass & CG team. The major responsibility is to collect and analyse general engine data and calculate mass and CG of the baseline aircraft. In the second stage, the author mainly focuses on calculating mass and CG of the flying wing configuration. Figure3-1 shows the general layout of FW-11.

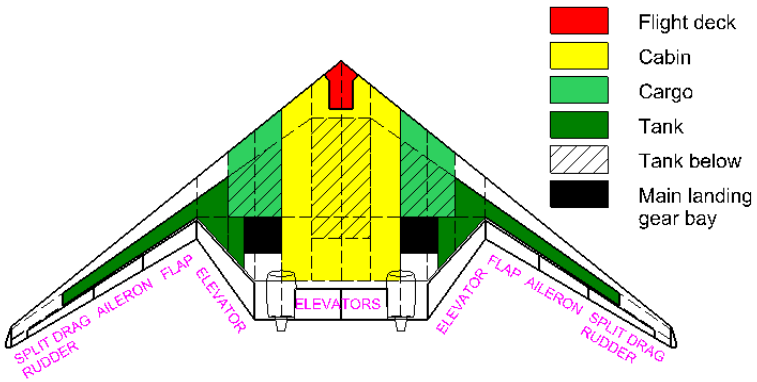

9-1 Layout of FW-11

In order to get reasonable inertia forces of FW-11, getting a more appropriate maximum takeoff weight (MTW) is very important. Because in this stage, quite a lot sub items are related to MTW, not only some mass breakdown items, but

also the other systems data like the engine and wing geometry. So it needs interaction calculation. The author put all the related data which is included mass , CG, landing gear, wing geometry, aerodynamic and engine into the same Excel. Then let MTW be the only variable figure and do the interaction calculation. Through this method, the maximum takeoff weight is more accurate.

A.2 Specification of Mass and CG

The main figures of mass & CG of FW-11 are described in table A_1 below.

A-1 Mass and CG specification

Design maximum take off mass	176469 kg
Operating empty mass	75044 kg
Design fuel load	72740 kg
Centre of gravity at OEM aft of fuselage apex	14.97 m
Centre of gravity range	0.307 to 0.446 MAC
Centre of gravity range at flight	0.307 to 0.371 MAC

Appendix B MATLAB code for static aeroelastic deformation

All the MATLAB code in the thesis requires the symbolic toolbox.

```
syms EI0  EI8 GJ0 GJ8 %stiffness data from BOXEM
EI0=0.40310E+09 %Bending stiffness of section 1
EI8=0.42284E+07 %Bending stiffness of section 8
GJ0=0.50920E+09 %Torsional stiffness of section 1
GJ8=0.61165E+07 %Torsional stiffness of section 8
%Geometry data from catia model
syms c0 c1 c2 c3 c4 c5 c6 c7 c8 la
c0=6 %The length of chord at the root of the outer wing,y=0
c8=2 % The length of chord at the tip of the outer wing,y=16
c1=c0-(c0-c8)/8 %the length of chord at y=2m
c2=c0-(c0-c8)/8*2 %the length of chord at y=4m
c3=c0-(c0-c8)/8*3 %the length of chord at y=6m
c4=c0-(c0-c8)/8*4 %the length of chord at y=8m
c5=c0-(c0-c8)/8*5 %the length of chord at y=10m
c6=c0-(c0-c8)/8*6 %the length of chord at y=12m
c7=c0-(c0-c8)/8*7 %the length of chord at y=14m
la=39/180*3.14 %the wing sweep angle
syms s1 s2 s3 s4 s5 s6 s7 s8 s
s1=(c0+c1)*2/2 %area of section 1
s2=c1+c2 %area of section 2
s3=c2+c3 %area of section 3
s4=c3+c4 %area of section 4
s5=c4+c5 %area of section 5
s6=c5+c6 %area of section 6
s7=c6+c7 %area of section 7
s8=c7+c8 %area of section 8
s=s1+s2+s3+s4+s5+s6+s7+s8 %area of the outer wing
syms y1 y2 y3 y4 y5 y6 y7 y8
y1=2 %distance of section 1 from the root of outer wing
y2=4 %distance of section 2 from the root of outer wing
y3=6 %distance of section 3 from the root of outer wing
```

```
y4=8 %distance of section 4 from the root of outer wing
y5=10 %distance of section 5 from the root of outer wing
y6=12 %distance of section 6 from the root of outer wing
y7=14 %distance of section 7 from the root of outer wing
y8=15.9 %distance of section 8 from the root of outer wing
syms m1 m2 m3 m4 m4 m5 m7 m8
%mass distribution of eight sections, with outer tank fuel
m1=1070.54
m2=795
m3=673
m4=561
m5=460
m6=368
m7=70
m8=14
syms alfa1 alfa2 alfa3 alfa4 alfa4 alfa6 alfa7 alfa8 alfa0
alfa0=1/180*3.14 % Initial AOA of the aircraft
% Initial AOA of each section
alfa1=alfa0
alfa2=alfa0
alfa3=alfa0
alfa4=alfa0
alfa5=alfa0
alfa6=alfa0
alfa7=alfa0
alfa8=alfa0
%aerodynamic data
syms D1 D2 D3 D4 D5 D6 D7 D8  den v
den=0.38 %density of the air at 35,000 ft
v=240.15 %speed of the aircraft at 35,00 ft
D1=den*(v^2)/2*s1
D2=den*(v^2)/2*s2
D3=den*(v^2)/2*s3
D4=den*(v^2)/2*s4
D5=den*(v^2)/2*s5
D6=den*(v^2)/2*s6
D7=den*(v^2)/2*s7
```

```
D8=den*(v^2)/2*s8
syms as ar y cm
ar=6 %Aspect ratio
as=0.19/3.1416*180 %Lift coefficient of the wing
cm=-0.00061/3.1416*180 %pitching moment coefficient of the wing
aw=as*(1-(y/16)^2) %modified method for lift distribution
syms cl1 cl2 cl3 cl4 cl5 cl6 cl7 cl8
%Lift coefficient of each section
cl1=as*(1-(y1/16)^2)*alfa1
cl2=as*(1-(y2/16)^2)*alfa2
cl3=as*(1-(y3/16)^2)*alfa3
cl4=as*(1-(y4/16)^2)*alfa4
cl5=as*(1-(y5/16)^2)*alfa5
cl6=as*(1-(y6/16)^2)*alfa6
cl7=as*(1-(y7/16)^2)*alfa7
cl8=as*(1-(y8/16)^2)*alfa8
%interation
%deformation from bending moment
syms F1 F2 F3 F4 F5 F6 F7 F8
syms f1 f2 f3 f4 f5 f6 f7 f8
syms w1d w2d w3d w4d w5d w6d w7d w8d
syms w1b w2b w3b w4b w5b w6b w7b w8b
syms ye1 ye2 ye3 ye4 ye5 ye6 ye7 ye8
syms thet1 thet2 thet3 thet4 thet5 thet6 thet7 thet8
%distance of each section from the root of outer wing at the elastic
axis
ye1=y1/cos(39/180*3.14)
ye2=y2/cos(39/180*3.14)
ye3=y3/cos(39/180*3.14)
ye4=y4/cos(39/180*3.14)
ye5=y5/cos(39/180*3.14)
ye6=y6/cos(39/180*3.14)
ye7=y7/cos(39/180*3.14)
ye8=y8/cos(39/180*3.14)
%forces of each section
F1=-D1*cl1*cos(alfa1)+m1*9.8
F2=-D2*cl2*cos(alfa2)+m2*9.8
```

```
F3=-D3*cl3*cos(alfa3)+m3*9.8
F4=-D4*cl4*cos(alfa4)+m4*9.8
F5=-D5*cl5*cos(alfa5)+m5*9.8
F6=-D6*cl6*cos(alfa6)+m6*9.8
F7=-D7*cl7*cos(alfa7)+m7*9.8
F8=-D8*cl8*cos(alfa8)+m8*9.8
syms mb1 mb2 mb3 mb4 mb5 mb6 mb7 mb8
syms mt1 mt2 mt3 mt4 mt5 mt6 mt7 mt8
%bending  moments of each section, using superpostion priciple
mb1=(F1+F2+F3+F4+F5+F6+F7+F8)*(y1-y)+(F2*(y2-y1)+F3*(y3-y1)+F4*(y4-
y1)+F5*(y5-y1)+F6*(y6-y1)+F7*(y7-y1)+F8*(y8-y1))
mb2=(F2+F3+F4+F5+F6+F7+F8)*(y2-y)+(F3*(y3-y2)+F4*(y4-y2)+F5*(y5-
y2)+F6*(y6-y2)+F7*(y7-y2)+F8*(y8-y2))
mb3=(F3+F4+F5+F6+F7+F8)*(y3-y)+(F4*(y4-y3)+F5*(y5-y3)+F6*(y6-
y3)+F7*(y7-y3)+F8*(y8-y3))
mb4=(F4+F5+F6+F7+F8)*(y4-y)+(F5*(y5-y4)+F6*(y6-y4)+F7*(y7-y4)+F8*(y8-
y4))
mb5=(F5+F6+F7+F8)*(y5-y)+(F6*(y6-y5)+F7*(y7-y5)+F8*(y8-y5))
mb6=(F6+F7+F8)*(y6-y)+F7*(y7-y6)+F8*(y8-y6)
mb7=(F7+F8)*(y7-y)+F8*(y8-y7)
mb8=F8*(y8-y)
%fuction of the elastic bending of each section
f1=(mb1*cos(la)-mt1*sin(la))/(EI0-(EI0-EI8)/y8*y1/2)
f2=(mb2*cos(la)-mt2*sin(la))/(EI0-(EI0-EI8)/y8*y2/2)
f3=(mb3*cos(la)-mt3*sin(la))/(EI0-(EI0-EI8)/y8*y3/2)
f4=(mb4*cos(la)-mt4*sin(la))/(EI0-(EI0-EI8)/y8*y4/2)
f5=(mb5*cos(la)-mt5*sin(la))/(EI0-(EI0-EI8)/y8*y5/2)
f6=(mb6*cos(la)-mt6*sin(la))/(EI0-(EI0-EI8)/y8*y6/2)
f7=(mb7*cos(la)-mt7*sin(la))/(EI0-(EI0-EI8)/y8*y7/2)
f8=(mb8*cos(la)-mt8*sin(la))/(EI0-(EI0-EI8)/y8*y8/2)
% bending slope of each section
thet1=int(f1,y,0,y)
thet2=thet1+int(f2,y,y1,y)
thet3=thet2+int(f3,y,y2,y)
thet4=thet3+int(f4,y,y3,y)
thet5=thet4+int(f5,y,y4,y)
thet6=thet5+int(f6,y,y5,y)
```

```
thet7=thet6+int(f7,y,y6,y)
thet8=thet7+int(f8,y,y7,y)
%bending deflection and  of each section
w1=int(thet1,y,0,y1)
w1b=int(thet1,y,0,ye1)
w1d=-w1+w1b
w2=int(thet2,y,y1,y2)
w2b=int(thet1,y,y1,ye2)
w2d=-w2+w2b
w3=int(thet3,y,y2,y3)
w3b=int(thet3,y,y2,ye3)
w3d=-w3+w3b
w4=int(thet4,y,y3,y4)
w4b=int(thet4,y,y3,ye4)
w4d=-w4+w4b
w5=int(thet5,y,y4,y5)
w5b=int(thet5,y,y4,ye5)
w5d=-w5+w5b
w6=int(thet6,y,y5,y6)
w6b=int(thet6,y,y5,ye6)
w6d=-w6+w6b
w7=int(thet7,y,y6,y7)
w7b=int(thet7,y,y6,ye7)
w7d=-w7+w7b
w8=int(thet8,y,y7,y8)
w8b=int(thet8,y,y7,ye8)
w8d=-w8+w8b
w8=vpa(w8,5)
w8b=vpa(w8b,5)
w1d=vpa(w1d,5)
w2d=vpa(w2d,5)
w3d=vpa(w3d,5)
w4d=vpa(w4d,5)
w5d=vpa(w5d,5)
w6d=vpa(w6d,5)
w7d=vpa(w7d,5)
w8d=vpa(w8d,5)
```

```
%AOA changed of each section by the bending moment
syms alfa1b alfa2b alfa3b alfa4b alfa5b alfa6b alfa7b alfa8b
alfa1b=atan(w1d/c1)
alfa1b=vpa(alfa1b,5)
alfa2b=atan(w2d/c2)
alfa2b=vpa(alfa2b,5)
alfa3b=atan(w3d/c3)
alfa3b=vpa(alfa3b,5)
alfa4b=atan(w4d/c4)
alfa4b=vpa(alfa4b,5)
alfa5b=atan(w5d/c5)
alfa5b=vpa(alfa5b,5)
alfa6b=atan(w6d/c6)
alfa6b=vpa(alfa6b,5)
alfa7b=atan(w7d/c7)
alfa7b=vpa(alfa7b,5)
alfa8b=atan(w8d/c8)
alfa8b=vpa(alfa8b,5)
% deformation from torsion moment
syms mtt1 mtt2 mtt3 mtt4 mtt5 mtt6 mtt7 mtt8
%torsion moment
mtt1=D1*cl1*0.1*c1+cm*alfa1*D1*c1
mtt2=D2*cl2*0.1*c2+cm*alfa2*D2*c2
mtt3=D3*cl3*0.1*c3+cm*alfa3*D3*c3
mtt4=D4*cl4*0.1*c4+cm*alfa4*D4*c4
mtt5=D5*cl5*0.1*c5+cm*alfa5*D5*c5
mtt6=D6*cl6*0.1*c6+cm*alfa6*D6*c6
mtt7=D7*cl7*0.1*c7+cm*alfa7*D7*c7
mtt8=D8*cl8*0.1*c8+cm*alfa8*D8*c8
%torsion moment of each section, useing superpostion principle
mt1=mtt1+mtt2+mtt3+mtt4+mtt5+mtt6+mtt7+mtt8
mt2=mtt2+mtt3+mtt4+mtt5+mtt6+mtt7+mtt8
mt3=mtt3+mtt4+mtt5+mtt6+mtt7+mtt8
mt4=mtt4+mtt5+mtt6+mtt7+mtt8
mt5=mtt5+mtt6+mtt7+mtt8
mt6=mtt6+mtt7+mtt8
mt7=mtt7+mtt8
```

```
mt8=mtt8
%deformation of the wing
syms T1 T2 T3 T4 T5 T6 T7 T8
syms g1 g2 g3 g4 g5 g6 g7 g8
%fuction of elastic torsion
T1=mt1*cos(la)+mb1*sin(la)
T2=mt2*cos(la)+mb2*sin(la)
T3=mt3*cos(la)+mb3*sin(la)
T4=mt4*cos(la)+mb4*sin(la)
T5=mt5*cos(la)+mb5*sin(la)
T6=mt6*cos(la)+mb6*sin(la)
T7=mt7*cos(la)+mb7*sin(la)
T8=mt8*cos(la)+mb8*sin(la)
g1=T1/(GJ0+(GJ8-GJ0)/y8*y1/2)
g2=T2/(GJ0+(GJ8-GJ0)/y8*y2/2)
g3=T3/(GJ0+(GJ8-GJ0)/y8*y3/2)
g4=T4/(GJ0+(GJ8-GJ0)/y8*y4/2)
g5=T5/(GJ0+(GJ8-GJ0)/y8*y5/2)
g6=T6/(GJ0+(GJ8-GJ0)/y8*y6/2)
g7=T7/(GJ0+(GJ8-GJ0)/y8*y7/2)
g8=T8/(GJ0+(GJ8-GJ0)/y8*y8/2)
%AOA changed by torsion moment
syms alfa1t alft2t alft3t alfa4t alfa5t alfa6t alfa7t alfa8t
alfa1t=int(g1,y,0,ye1)
alfa2t=int(g2,y,ye1,ye2)
alfa3t=int(g3,y,ye2,ye3)
alfa4t=int(g4,y,ye3,ye4)
alfa5t=int(g5,y,ye4,ye5)
alfa6t=int(g6,y,ye5,ye6)
alfa7t=int(g7,y,ye6,ye7)
alfa8t=int(g8,y,ye7,ye8)
alfa1t=vpa(alfa1t,5)
alfa2t=vpa(alfa2t,5)
alfa3t=vpa(alfa3t,5)
alfa4t=vpa(alfa4t,5)
alfa5t=vpa(alfa5t,5)
alfa6t=vpa(alfa6t,5)
```

```
alfa7t=vpa(alfa7t,5)
alfa8t=vpa(alfa8t,5)
%AOA changed from elastic bending and torsion
alfa0=vpa(alfa0,5)
alfa1=alfa1b+alfa1t+alfa0
alfa2=alfa2b+alfa2t+alfa0
alfa3=alfa3b+alfa3t+alfa0
alfa4=alfa4b+alfa4t+alfa0
alfa5=alfa5b+alfa5t+alfa0
alfa6=alfa6b+alfa6t+alfa0
alfa7=alfa7b+alfa7t+alfa0
alfa8=alfa8b+alfa8t+alfa0
%interaction calculation, repeat the method above, the number of times
of repeating is based on the error, cosidering the model gets the
equilibrium condition when the error less than 1%, in this case , the
number of times is 99.
syms alfa10 alfa20 alfa30 afla40 alfa50 alfa60 alfa70 alfa80
alfa10=alfa0
alfa20=alfa0
alfa30=alfa0
alfa40=alfa0
alfa50=alfa0
alfa60=alfa0
alfa70=alfa0
alfa80=alfa0
sum=0
for i=1:99
cl1=as*(1-(y1/16)^2)*alfa1
cl2=as*(1-(y2/16)^2)*alfa2
cl3=as*(1-(y3/16)^2)*alfa3
cl4=as*(1-(y4/16)^2)*alfa4
cl5=as*(1-(y5/16)^2)*alfa5
cl6=as*(1-(y6/16)^2)*alfa6
cl7=as*(1-(y7/16)^2)*alfa7
cl8=as*(1-(y8/16)^2)*alfa8
syms F1 F2 F3 F4 F5 F6 F7 F8
syms f1 f2 f3 f4 f5 f6 f7 f8
```

```
syms w1d w2d w3d w4d w5d w6d w7d w8d
syms w1b w2b w3b w4b w5b w6b w7b w8b
syms ye1 ye2 ye3 ye4 ye5 ye6 ye7 ye8
syms thet1 thet2 thet3 thet4 thet5 thet6 thet7 thet8
y1=2
y2=4
y3=6
y4=8
y5=10
y6=12
y7=14
y8=16
ye1=y1/cos(39/180*3.14)
ye2=y2/cos(39/180*3.14)
ye3=y3/cos(39/180*3.14)
ye4=y4/cos(39/180*3.14)
ye5=y5/cos(39/180*3.14)
ye6=y6/cos(39/180*3.14)
ye7=y7/cos(39/180*3.14)
ye8=y8/cos(39/180*3.14)
F1=-D1*cl1*cos(alfa1)+m1*9.8
F2=-D2*cl2*cos(alfa2)+m2*9.8
F3=-D3*cl3*cos(alfa3)+m3*9.8
F4=-D4*cl4*cos(alfa4)+m4*9.8
F5=-D5*cl5*cos(alfa5)+m5*9.8
F6=-D6*cl6*cos(alfa6)+m6*9.8
F7=-D7*cl7*cos(alfa7)+m7*9.8
F8=-D8*cl8*cos(alfa8)+m8*9.8
syms mb1 mb2 mb3 mb4 mb5 mb6 mb7 mb8
syms mt1 mt2 mt3 mt4 mt5 mt6 mt7 mt8
mb1=(F1+F2+F3+F4+F5+F6+F7+F8)*(y1-y)+(F2*(y2-y1)+F3*(y3-y1)+F4*(y4-
y1)+F5*(y5-y1)+F6*(y6-y1)+F7*(y7-y1)+F8*(y8-y1))
mb2=(F2+F3+F4+F5+F6+F7+F8)*(y2-y)+(F3*(y3-y2)+F4*(y4-y2)+F5*(y5-
y2)+F6*(y6-y2)+F7*(y7-y2)+F8*(y8-y2))
mb3=(F3+F4+F5+F6+F7+F8)*(y3-y)+(F4*(y4-y3)+F5*(y5-y3)+F6*(y6-
y3)+F7*(y7-y3)+F8*(y8-y3))
mb4=(F4+F5+F6+F7+F8)*(y4-y)+(F5*(y5-y4)+F6*(y6-y4)+F7*(y7-y4)+F8*(y8-
```

```
y4))
mb5=(F5+F6+F7+F8)*(y5-y)+(F6*(y6-y5)+F7*(y7-y5)+F8*(y8-y5))
mb6=(F6+F7+F8)*(y6-y)+F7*(y7-y6)+F8*(y8-y6)
mb7=(F7+F8)*(y7-y)+F8*(y8-y7)
mb8=F8*(y8-y)
syms mtt1 mtt2 mtt3 mtt4 mtt5 mtt6 mtt7 mtt8
mtt1=D1*cl1*0.1*c1+cm*alfa1*D1*c1
mtt2=D2*cl2*0.1*c2+cm*alfa2*D2*c2
mtt3=D3*cl3*0.1*c3+cm*alfa3*D3*c3
mtt4=D4*cl4*0.1*c4+cm*alfa4*D4*c4
mtt5=D5*cl5*0.1*c5+cm*alfa5*D5*c5
mtt6=D6*cl6*0.1*c6+cm*alfa6*D6*c6
mtt7=D7*cl7*0.1*c7+cm*alfa7*D7*c7
mtt8=D8*cl8*0.1*c8+cm*alfa8*D8*c8
mt1=mtt1+mtt2+mtt3+mtt4+mtt5+mtt6+mtt7+mtt8
mt2=mtt2+mtt3+mtt4+mtt5+mtt6+mtt7+mtt8
mt3=mtt3+mtt4+mtt5+mtt6+mtt7+mtt8
mt4=mtt4+mtt5+mtt6+mtt7+mtt8
mt5=mtt5+mtt6+mtt7+mtt8
mt6=mtt6+mtt7+mtt8
mt7=mtt7+mtt8
mt8=mtt8
f1=(mb1*cos(la)-mt1*sin(la))/(EI0-(EI0-EI8)/y8*y1/2)
f2=(mb2*cos(la)-mt2*sin(la))/(EI0-(EI0-EI8)/y8*y2/2)
f3=(mb3*cos(la)-mt3*sin(la))/(EI0-(EI0-EI8)/y8*y3/2)
f4=(mb4*cos(la)-mt4*sin(la))/(EI0-(EI0-EI8)/y8*y4/2)
f5=(mb5*cos(la)-mt5*sin(la))/(EI0-(EI0-EI8)/y8*y5/2)
f6=(mb6*cos(la)-mt6*sin(la))/(EI0-(EI0-EI8)/y8*y6/2)
f7=(mb7*cos(la)-mt7*sin(la))/(EI0-(EI0-EI8)/y8*y7/2)
f8=(mb8*cos(la)-mt8*sin(la))/(EI0-(EI0-EI8)/y8*y8/2)
syms T1 T2 T3 T4 T5 T6 T7 T8
syms g1 g2 g3 g4 g5 g6 g7 g8
T1=mt1*cos(la)+mb1*sin(la)
T2=mt2*cos(la)+mb2*sin(la)
T3=mt3*cos(la)+mb3*sin(la)
T4=mt4*cos(la)+mb4*sin(la)
T5=mt5*cos(la)+mb5*sin(la)
```

```
T6=mt6*cos(la)+mb6*sin(la)
T7=mt7*cos(la)+mb7*sin(la)
T8=mt8*cos(la)+mb8*sin(la)
g1=T1/(GJ0+(GJ8-GJ0)/y8*y1/2)
g2=T2/(GJ0+(GJ8-GJ0)/y8*y2/2)
g3=T3/(GJ0+(GJ8-GJ0)/y8*y3/2)
g4=T4/(GJ0+(GJ8-GJ0)/y8*y4/2)
g5=T5/(GJ0+(GJ8-GJ0)/y8*y5/2)
g6=T6/(GJ0+(GJ8-GJ0)/y8*y6/2)
g7=T7/(GJ0+(GJ8-GJ0)/y8*y7/2)
g8=T8/(GJ0+(GJ8-GJ0)/y8*y8/2)
thet1=int(f1,y,0,y)
thet2=thet1+int(f2,y,y1,y)
thet3=thet2+int(f3,y,y2,y)
thet4=thet3+int(f4,y,y3,y)
thet5=thet4+int(f5,y,y4,y)
thet6=thet5+int(f6,y,y5,y)
thet7=thet6+int(f7,y,y6,y)
thet8=thet7+int(f8,y,y7,y)
w1=int(thet1,y,0,y1)
w1b=int(thet1,y,0,ye1)
w1d=-w1+w1b
w2=int(thet2,y,y1,y2)
w2b=int(thet1,y,y1,ye2)
w2d=-w2+w2b
w3=int(thet3,y,y2,y3)
w3b=int(thet3,y,y2,ye3)
w3d=-w3+w3b
w4=int(thet4,y,y3,y4)
w4b=int(thet4,y,y3,ye4)
w4d=-w4+w4b
w5=int(thet5,y,y4,y5)
w5b=int(thet5,y,y4,ye5)
w5d=-w5+w5b
w6=int(thet6,y,y5,y6)
w6b=int(thet6,y,y5,ye6)
w6d=-w6+w6b
```

```
w7=int(thet7,y,y6,y7)
w7b=int(thet7,y,y6,ye7)
w7d=-w7+w7b
w8=int(thet8,y,y7,y8)
w8b=int(thet8,y,y7,ye8)
w8d=-w8+w8b
w8=vpa(w8,5)
w8b=vpa(w8b,5)
w1d=vpa(w1d,5)
w2d=vpa(w2d,5)
w3d=vpa(w3d,5)
w4d=vpa(w4d,5)
w5d=vpa(w5d,5)
w6d=vpa(w6d,5)
w7d=vpa(w7d,5)
w8d=vpa(w8d,5)
syms alfa1b alfa2b alfa3b alfa4b alfa5b alfa6b alfa7b alfa8b
alfa1b=atan(w1d/c1)
alfa1b=vpa(alfa1b,5)
alfa2b=atan(w2d/c2)
alfa2b=vpa(alfa2b,5)
alfa3b=atan(w3d/c3)
alfa3b=vpa(alfa3b,5)
alfa4b=atan(w4d/c4)
alfa4b=vpa(alfa4b,5)
alfa5b=atan(w5d/c5)
alfa5b=vpa(alfa5b,5)
alfa6b=atan(w6d/c6)
alfa6b=vpa(alfa6b,5)
alfa7b=atan(w7d/c7)
alfa7b=vpa(alfa7b,5)
alfa8b=atan(w8d/c8)
alfa8b=vpa(alfa8b,5)
%elastic torsion
syms alfa1t alft2t alft3t alfa4t alfa5t alfa6t alfa7t alfa8t
alfa1t=int(g1,y,0,ye1)
alfa2t=int(g2,y,ye1,ye2)
```

```
alfa3t=int(g3,y,ye2,ye3)
alfa4t=int(g4,y,ye3,ye4)
alfa5t=int(g5,y,ye4,ye5)
alfa6t=int(g6,y,ye5,ye6)
alfa7t=int(g7,y,ye6,ye7)
alfa8t=int(g8,y,ye7,ye8)
alfa1t=vpa(alfa1t,5)
alfa2t=vpa(alfa2t,5)
alfa3t=vpa(alfa3t,5)
alfa4t=vpa(alfa4t,5)
alfa5t=vpa(alfa5t,5)
alfa6t=vpa(alfa6t,5)
alfa7t=vpa(alfa7t,5)
alfa8t=vpa(alfa8t,5)
alfa12=alfa1b+alfa1t+alfa1
alfa22=alfa2b+alfa2t+alfa2
alfa32=alfa3b+alfa3t+alfa3
alfa42=alfa4b+alfa4t+alfa4
alfa52=alfa5b+alfa5t+alfa5
alfa62=alfa6b+alfa6t+alfa6
alfa72=alfa7b+alfa7t+alfa7
alfa82=alfa8b+alfa8t+alfa8
alfa10=alfa1
alfa1=alfa12
alfa20=alfa2
alfa2=alfa22
alfa30=alfa3
alfa3=alfa32
alfa40=alfa4
alfa4=alfa42
alfa50=alfa5
alfa5=alfa52
alfa60=alfa6
alfa6=alfa62
alfa70=alfa7
alfa7=alfa72
alfa80=alfa8
```

```
alfa8=alfa82
sum=sum+1
end
%AFter the iteraction calculation, the AOA of each section
alfa0=vpa(alfa0,5)
alfa1=vpa(alfa1,5)
alfa2=vpa(alfa2,5)
alfa3=vpa(alfa3,5)
alfa4=vpa(alfa4,5)
alfa5=vpa(alfa5,5)
alfa6=vpa(alfa6,5)
alfa7=vpa(alfa7,5)
alfa8=vpa(alfa8,5)
```

Appendix C MATLAB code for rolling effectiveness estimation

C.1 Rolling effectiveness for rigid aircraft

```
syms den v0 q cd
den=0.38 %density of air at 35,000 ft
v0=243.15 %velocity of the cruise condition
q=den*(v0^2)/2 % dynamic pressure
cd=0.00744 %drag coefficient
syms as  y cm aw
as=0.19/3.1416*180 %slope of lift coefficient
cm=-0.00061/3.1416*180 %pitch moment coeffient
aw=as*(1-(y/16)^2)%modified parameter for the slope of lift
coefficient
%Geometry data from catia model
syms c0 c1 c2 c3 c4 c5 c6 c7 c8 la
c0=6 %The length of chord at the root of the outer wing,y=0
c8=2 % The length of chord at the tip of the outer wing,y=16
c1=c0-(c0-c8)/8 %the length of chord at y=2m
c2=c0-(c0-c8)/8*2 %the length of chord at y=4m
c3=c0-(c0-c8)/8*3 %the length of chord at y=6m
c4=c0-(c0-c8)/8*4 %the length of chord at y=8m
c5=c0-(c0-c8)/8*5 %the length of chord at y=10m
c6=c0-(c0-c8)/8*6 %the length of chord at y=12m
c7=c0-(c0-c8)/8*7 %the length of chord at y=14m
la=39/180*3.14 %the wing sweep angle
syms f1 f2 f3 f4 f5 f6 f7 f8
syms p
f1=q*c1*(aw+cd)*y^2/v0
f2=q*c2*(aw+cd)*y^2/v0
f3=q*c3*(aw+cd)*y^2/v0
f4=q*c4*(aw+cd)*y^2/v0
f5=q*c5*(aw+cd)*y^2/v0
f6=q*c6*(aw+cd)*y^2/v0
f7=q*c7*(aw+cd)*y^2/v0
```

```
f8=q*c8*(aw+cd)*y^2/v0
syms lp1 lp2 lp3 lp4 lp5 lp6 lp7 lp8 lp
%Rolling moment derivative due to the roll rate of each section
lp1=-2*int(f1,y,0,2)
lp2=-2*int(f2,y,2,4)
lp3=-2*int(f3,y,4,6)
lp4=-2*int(f4,y,6,8)
lp5=-2*int(f5,y,8,10)
lp6=-2*int(f6,y,10,12)
lp7=-2*int(f7,y,12,14)
lp8=-2*int(f8,y,14,16)
lp=lp1+lp2+lp3+lp4+lp5+lp6+lp7+lp8
lp=vpa(lp,5) %Rolling moment derivative due to the roll rate of outer
wing
syms ac
ac=0.123*180/3.14 %slope of lift coefficient of the aileron
syms r
syms g1 g2 g3 g4 g5 g6 g7 g8
g1=q*c1*ac*y
g2=q*c2*ac*y
g3=q*c3*ac*y
g4=q*c4*ac*y
g5=q*c5*ac*y
g6=q*c6*ac*y
g7=q*c7*ac*y
g8=q*c8*ac*y
syms lr1 lr2 lr3 lr4 lr5 lr6 lr7 lr8 lr
%Rolling moment derivative due to aileron
lr3=2*int(g3,y,4,6)
lr4=2*int(g4,y,6,8)
lr=lr3+lr4
lr=vpa(lr,5)
syms Ix
Ix=3430236 %moment of inertia roll
p_r=-lr/lp
ezplot(p_r,[0 10]) %roll rate per aileron
figure
```

```
syms pt t
r0=2 %deflection of aileron
pt=-lr/lp*(1-exp(lp/Ix*t))*r0 %the transient roll rate response
ezplot(pt,[0,50])
```

C.2 Rolling effectiveness for flexible aircraft

```
clc
clear
syms d v0 q cd
d=0.38 %density of the air at 35,000ft
cd=0.00744 %Drag coefficient
syms as  y cm aw
as=0.19/3.1416*180 %lift coeffiecient slope
faw=(1-(y/16)^2) % modified strip method parameter
aw=int(faw,y,0,16)/16*as
aw=vpa(aw,5)%modified lift coeffiecient slope of the wing
ac=int(faw,y,0,16)/16*0.123/3.1416*180
ac=vpa(ac,5)%modified lift coeffiecient slope of the flap, aileron
syms Ix
Ix=10391139 %moment of inertia roll
syms sw c ac s me la law
me=122466/3 %the modal mass
s=16 %span of the wing
sw=64 %area of the wing
sr=18 %area of the aileron
c=4 %chord length of the wing
ac=4.6982 %slope of lift coefficient of aileron
% v0=240, cruise speed
syms lp lr le
lp=-0.5*d*v0*sw*(aw+cd)*s*s/3 %Rolling moment derivative due to the
roll rate
lr=0.5*d*v0^2*sr*ac*s/2 %Rolling moment derivative due to aileron
le=-0.5*d*v0^2*sw*aw*s/3 %the rolling moment due to flexible mode
deformation
syms qp qr qe
qp=0.5*d*v0*sw*aw*la*s/3 %the flexible mode generalized force due to
the roll rate
```

```
qr=0.5*d*v0^2*sr*ac*(law-la)*0.5 %the flexible mode generalized force
due to the deflection of the aileron
qe=0.5*d*v0^2*sw*aw*la/3 %the flexible mode generalized force due to
flexible mode deformation
syms ke wn  ksi ce
wn=8 %natural frequency
ke=me*wn^2 %stiffness
ksi=0.04 %damping modal
ce=ksi*2*me*wn %damping
syms f_ef_f f_ef_r r
%aileron effectiveness
f_ef_r=-lr/lp
f_ef_f=(lr*(ke-qe)+le*qr)/(-lp*(ke-qe)-le*qp)
r=f_ef_f/f_ef_r
ezplot(r,[0 250])
figure
%transient roll rate response
[T,Y] = ode45(@dydt_with,[0 30],[0 0 0 0]);
plot(T,Y(:,2),'-')
xlabel('Time(s)'); ylabel('Roll Rate(deg/s) ');
legend('Roll rate')
 %%%%%%%%%%%%%%%%%%%%%%%%%%%%%%%%%%%%%%%%%%%%%%%%%%%%%%%%%%%%%%%%%%%%%%%%%%%%
function dy=dydyt(t,y)
dy = zeros(4,1);
dy(1)=y(2) %roll rate
dy(2) = (-1.7918e+006*y(2) -2.7792e+007*y(3)+1.5e7*2)/10391139
%roll acceleration
dy(3) = y(4) %flexible deformation
dy(4)=(4.5749e+004*y(2)+7.4041e+005*2*2- 2.6126e+004*y(4)-(2612608-
2.2259e5)*y(3))/(122466/3)
%slope of flexible deformation

% dy(1) = (lp*y(1) +le*y(2)+lr*r)/Ix
% dy(4)=(qp*y(1)+qr*r-ce*y(4)-(ke-qe)*y(3))/me
%one example of input data
% lp = -1.8092e+006
% lr =  7.4041e+006
```

```
% le = -2.7110e+007
% qp =  4.5184e+004
% qr =  7.4041e+005
% qe =  2.2259e5
% wn =  8
% ke =  2612608
% ksi = 0.0400
% ce =  2.6126e+004
```